C.P. No. 872

C.P. No. 872

MINISTRY OF AVIATION

AERONAUTICAL RESEARCH COUNCIL

CURRENT PAPERS

Viscosity Effects on the Two-Dimensional Flow in Cascades

By

J. P. Gostelow, A. K. Lewkowicz and

M. R. A. Shaalan

LONDON: HER MAJESTY'S STATIONERY OFFICE

1967

Price 8s. 6d. net

C.P. No.872*

October, 1965

Viscosity Effects on the Two-Dimensional Flow in Cascades

- By -
J. P. Gostelow, A. K. Lewkowicz
and M. R. A. Shaalan

SUMMARY

An outline of three methods selected for boundary layer calculation is given. One of these methods is a new analysis. The methods are programmed in ALGOL-code and the results obtained are graphically displayed. Both theoretical and experimental velocity distributions are used in the computation.

Results obtained from the new analysis are compared with those from other methods and also with experimental measurements.

Applying boundary layer theory, an attempt is made to reveal the real effect of viscosity on pressure distributions in cascades.

The method developed is briefly described and the results obtained are compared with experiment.

*Replaces ULME/B.13 - A.R.C.27 209

1. INTRODUCTION

Information on the effect of viscosity on two dimensional cascade flow and on its influence on the performance of real turbomachines is surprisingly scanty. The subject matter of the present report is brought together from two extensive research programmes:

(i) study of the potential flow past two dimensional cascades.
(ii) study of boundary layer flow.

It is commonly appreciated that an analytical solution to the complete Navier-Stokes equations for cascade flows is analytically impossible and thus approximate approaches to the viscous flow past two dimensional cascades have to be sought. The simplest way of attacking the problem is to correct the potential flow solution for the effect of the boundary layer in an iterative manner. The available potential flow calculation provides necessary information for boundary layer calculations and consequently should be capable of incorporating boundary layer corrections for the second approximation. The convergence of the iterative process is expected to be rapid.

Many potential flow investigators assume a cusped trailing edge and apply the Kutta condition in order to predict lift coefficient, outlet angle and pressure distribution. This is not compatible with current practical applications where most of the cascades have rounded leading and trailing edges. In such instances the Kutta condition is not relevant and for any given cascade geometry and inlet flow conditions, the outlet flow conditions depend on the location of the rear stagnation point. From the standpoint of potential flow theory there is no definite way of prescribing the location of the rear stagnation point and therefore some suppositions must be made from the state of boundary layer development at the trailing edge and from the development of the profile wake further downstream. The quest for such an alternative to the Kutta condition is described in Section 5 of the present report.

On the other hand, the presence of the boundary layer in the actual aerofoil acts as if altering its shape and thus affecting the state of potential flow. By adding the boundary layer displacement thickness to the profile thickness along the normals to its contour, account is taken of the effect of viscosity on this "change in shape" of the aerofoils in cascades. The first use of this procedure was probably by Pinkerton (11) who worked back from the measured circulation to determine an arbitrary new profile by distortion of the aerofoil trailing edge. However, a complete solution of the problem would not have required the specification of an experimentally determined lift coefficient. Preston (12) firstly overcame this difficulty and was also able to correct for the displacement effect of the boundary layer on the flow around an isolated aerofoil. Preston's results gave excellent agreement with experimental measurements.

Spiedel and Scholz (14) first achieved an extension to cascades using the potential flow theory of Schlichting (13) and the boundary layer theory of Truckunbrodt. They were able to calculate the boundary layer as far as the separation point and to express the effect of the displacement thickness in terms of an additional source-sink distribution. The result of adding the displacement thickness was a 'substitute' profile which differed from the original profile by having its cusped trailing edge in a slightly different position. The displacement effect of the wake was not taken into account. The potential flow around the new profile was calculated, the rear stagnation point being fixed on the cusp by the Kutta condition. In a very thorough piece of work they applied corrections to a wide range of cascades and compared the results with experimental pressure distributions, outlet angles and loss coefficients.

A reliable calculation of the development of boundary layer on the considered aerofoil in cascade is obviously essential. In the present report some methods of calculation are described and their utility illustrated in several experimental as well as some hypothetical cases. Those methods being in current use in the University of Liverpool and also quoted in the present report are:

(i) Thwaites' method for laminar layers
(ii) Truckenbrodt's method for turbulent layers.
(iii) A new analysis (Lewkowicz and Horlock (7)) for turbulent layers.

However, the calculation of the boundary layer on an aerofoil is strongly influenced by the state of transition from laminar to turbulent boundary layer flow and moreover, to a greater degree, by its exact location. The transition location pertinent to cascade flows is undoubtedly one of the least explored problems in the theory of turbomachines. It should be emphasised that the existing experimental criteria for transition apply to much higher Reynolds numbers and lower turbulence levels than those encountered in cascade practice where often the transition is caused by laminar separation bubbles. An analytical prediction of the boundary layer downstream of the separation bubble appears to be intractable as yet.

Throughout the present report the following general assumptions are maintained:

(i) the flow is incompressible
(ii) the flow is steady
(iii) the effect of viscosity can be limited to a narrow region near the solid walls - the boundary layer region.

They naturally restrict the application of the present considerations, but nonetheless, it is hoped that the evidence discussed may be helpful in understanding the physics of viscous flow through turbomachinery cascades.

2. NOTATION

A.V.R.	Axial velocity ratio (outlet axial velocity/inlet axial velocity)
C_p	$= (p - p_1)/ \ 1/2 \ \rho U_1^2$ - local static pressure coefficient
ΔC_p	$= C_{ps} - C_{pP}$
H	$= \delta^*/\theta$ mean velocity shape parameter.
$\bar{H}$	$= \delta^{**}/\theta$ mean velocity shape parameter.
L	For parameter in Truckenbrodt's method or a function of ℓ and m in Thwaites' method.
a_{ij}	($i = 1, 2, 3$: $j = 1, 2, 3$) - functions of ω, δ and Π.
a_{4j}	($j = 1, 2, 3$) - functions of ω, δ, Π and $\frac{2}{U_\infty}\frac{dU_\infty}{dx}$
R_θ	Momentum thickness Reynolds Number, $R_\theta = \frac{U_\infty \theta}{\nu}$
R_e	Reynolds Number, $R_e = \frac{U_1 c}{\nu}$
S	Source distribution in Horlock's method.
U	Velocity (in the boundary layer region).
c	Blade chord length
c_f	Local skin friction coefficient
ℓ, m	Functions defined in Thwaites' method.
p	Static pressure (local value).
u_τ	Skin friction velocity.
x	Longitudinal coordinate (along the wall or along chord in low cambered blades).
y	Traverse coordinate (across boundary layer or normal to chord in low cambered blades)
z	$= x + iy$ complex variable in cascade plane.

a	Constant in the new analysis or flow angle in potential flow considerations.
δ	Absolute thickness of the boundary layer.
δ^*	Displacement thickness of the boundary layer.
δ^{**}	Energy thickness of the boundary layer
θ	Momentum thickness of the boundary layer
ω	$= \sqrt{c_f/2}$ local skin friction coefficient
ν	Kinematic viscosity of the fluid
σ	Stagger angle
τ	$= \rho(\overline{-uv})$ turbulent shear stress.
Π	Free parameter (Coles' parameter).
$\frac{2}{U_\infty} \cdot \frac{dU_\infty}{dx}$	External pressure gradient.

SUBSCRIPTS

T	In the trailing edge plane.
τ	Surface value
S	On the suction surface
P	On the pressure
o	Initial value
1	Inlet conditions (far upstream)
2	Outlet conditions (far downstream)
∞	Free stream value (outside boundary layer)

3. Methods of Boundary Layer Calculation in Use at Liverpool University.

3.1. Synopsis of Methods:

Various methods are available for the calculation of the boundary layer growth along a specified wall shape. Of the available methods, that of Thwaites (18) was chosen as a quick method for calculating the laminar part of the boundary layer. Truckenbrodt's (19) method was used to calculate the turbulent region of the boundary layer either starting at the laminar separation point or with assumed transition position and suitable initial values of shape parameter H and momentum thickness Reynolds Number R_θ.

A method recently developed by Lewkowicz and Horlock (7) was used and compared with other methods.

A brief description of the individual methods is given below:

3.1.1. The "Thwaites" Method

Starting with the momentum equation, Thwaites defined parameters ℓ and m to establish a relationship between the first and second derivatives of the velocity profile at the wall.

With these definitions, he succeeded in integrating the momentum equation, obtaining an expression for the momentum thickness θ. The shape parameter H (m) and a quantity L (a function of ℓ and m) were tabulated against the parameter m, so that for a value of m, values of L and H could be obtained.

As ℓ (m) is directly proportional to the velocity profile gradient at the wall, separation occurs when ℓ (m) becomes zero, at which the corresponding value of m is 0.082. This value of m at separation has since been corrected to 0.09 experimentally by Curle and Skan.

3.1.2. The "Truckenbrodt" Method

This method has been shown to be one of the most reliable methods for turbulent boundary layer calculation. The method is also relatively easy to apply since specification of the free stream velocity gradient is not required. The method is valid for plane and axi-symmetric flows with zero, favourable and/or adverse pressure gradient.

Manipulation of the energy integral equation, with the aid of semi-empirical relations between: the energy "dissipation" and R_θ, the wall shear stress, the shape parameter H and R_θ, and between H and $\bar{H}$ ($\frac{\text{energy thickness}}{\text{momentum thickness}}$), led to an expression for the momentum thickness θ. Again, using the energy integral

equation together with the momentum integral equation a formula for a form parameter L, which is a function of H, was reached.

Ludweig and Tillman's results of the wall shearing stress were used to give an equation for calculation of the skin friction coefficient.

Truckenbrodt considered c_f to be sufficiently small when H takes the value 2.4, for separation to occur.

A value of H = 1.4 immediately after transition was proposed by Truckenbrodt although it was possible to calculate this value as a function of the values of R_θ and H at laminar separation.

3.1.3. New Analysis

If it is taken for granted that the mean velocity profile in a two dimensional turbulent boundary layer can adequately be described by Coles' profile (2) then the development of the boundary layer is conveniently expressed in terms of three local variables:

(i) skin friction coefficient c_f, or $\omega = \sqrt{c_f/2}$,
(ii) free parameter (pertinent to the wake component) Π ,
(iii) absolute boundary layer thickness δ . (*)

All boundary layer mean velocity quantities e.g. δ^*, θ, δ^{**}, $H = \delta^*/\theta$ and $\bar{H} = \delta^{**}/\theta$ usually required in practical computations are also easily expressible by the three local variables of turbulent boundary layers. In the present report only a few remarks about the analysis will be made for further details the reader is referred to (7).

The new analysis is based on the three known boundary layer relations:

(i) momentum integral equation,
(ii) energy integral equation,
(iii) Ludwieg and Tillman skin friction law.

The number of the governing equations is dictated by the number of unknowns (local variables c_f, δ , Π). The governing equations are transformed into a set of three ordinary differential equations of first order for c_f, δ , and Π , on expressing all corresponding boundary layer integral quantities by the independent variables. All the three equations bear the same general form

---

Footnote.

(*) The absolute thickness of the boundary layer is here uniquely defined by the relation

$$\delta = \frac{k}{\omega} \frac{\delta^*}{(1 + \Pi)} \quad ; \quad \text{(where } k \text{ is the v.Kármán constant)}$$

which represents an immediate consequence of Coles' velocity profile.

$$\frac{d\omega}{dx} a_{1i} + \frac{d\delta}{dx} a_{2i} + \frac{d\Pi}{dx} a_{3i} = a_{4i}; \quad (i = 1,2,3); \qquad \ldots (1)$$

where a_{1i}, a_{2i}, a_{3i} are functions of ω, δ, Π and a_{4i} besides the local variables contains also the external pressure gradient $(2/U_\infty) \cdot (dU_\infty/dx)$ which initially is a known function of x.

Note that the Ludwieg and Tillman skin friction law must be differentiated with respect to x in order to complete the set of differential equations. This is essential because the solution to the set of equations is carried out numerically using the Runge-Kutta method for a system of first order differential equations to be solved simultaneously.

The energy integral equation contains a term involving turbulent shear stresses $\tau = \rho(-\overline{uv})$ in the state of energy dissipation integral

$$\int_0^\infty \frac{\tau}{\rho} \frac{\partial U}{\partial y} dy; \qquad \ldots (2)$$

This energy "dissipation" integral is related to the local variables by making use of Clauser's eddy viscosity model (1). Lewkowicz and Horlock (7) obtained an explicit relation for the energy "dissipation" integral *).

In order to make the new analysis reasonably accurate near separation the influence of the turbulent normal stresses is taken into consideration in the momentum balance (momentum integral equation). The role of the turbulent normal stresses, however, is omitted in the mean flow energy balance (energy integral equation). It is believed that the contribution of the turbulent normal stresses to the energy balance can be ignored even in the vicinity of separation.

Footnote

*) The dissipation integral depends on the constant a which takes its origin from the expression for the eddy viscosity in the outer region of a turbulent boundary layer. For further details refer to (1) and (7).

3.2. Computational Procedures

3.2.1. Methods of Thwaites and Truckenbrodt

Computer programs have been written in ALGOL-code to predict the behaviour of the boundary layer under particular pressure distributions using the methods described above. A separate program was prepared for Thwaites' method and an application was made to an experimental pressure distribution on the suction surface of low cambered aerofoils in a two dimensional cascade with the value of the axial velocity ratio maintained at unity. The point of laminar separation was predicted using Thwaites' criterion ($m_s = 0.082$) and alternatively by the use of Curle and Skan corrected value ($m = 0.090$).

Results of both criteria are shown in Fig. 13.

The same computer language was used to write a program for Truckenbrodt's method with a suitable transition point assumption. The point of turbulent separation was obtained using the value 2.4 for H at separation.

Programs for Thwaites' and Truckenbrodt's methods were combined to constitute a program which can be used to compute the boundary layer variables commencing with the flow laminar from a certain point and becoming turbulent under certain circumstances - convenient transition assumptions were made either at laminar separation point or at any other point arbitrarily chosen. The program provides for repitition of the whole calculation for different values of Reynolds number.

Fig. 1.a gives a flow diagram of the combined program.

3.2.2. The New Analysis

The Runge-Kutta method is selected for the numerical solution, primarily on account of its availability in the state of a ready to use procedure on a high speed electronic computer, and secondly because it is versatile and also has generally favourable characteristics of stability.

The Runge-Kutta method requires that the initial conditions are known and in particular that the solved equations are expressible in the following form

$$\frac{dy_i}{dx} = f(y_i, x) ; \quad i = 1, 2, 3.$$

In order to fulfil the requirement that all the derivatives $d\omega/dx$, $d\delta/dx$, and $d\Pi/dx$ be alone on the right hand side of the differential equations the set of equations (1) should be solved as a system of algebraic equations treating the derivatives as unknowns. The determinant method can conveniently be used for this purpose.

The corresponding computer program has been written in two different codes: Alpha-code to be used on the English Electric DEUCE computer and Liverpool University ALGOL - code, suitable for the much faster English Electric KDF-9 machine. The machine time consumed for the actual computation is approximately 45 sec. per step on the DEUCE-computer and only 5 sec. per step on the KDF 9 machine. The general flow diagram of the computer program is given in Fig. 1.b.

4. General Interpretation of Results Obtained

4.1. Application of Trückenbrodt Method Program

Smith (16) reviewed various methods of turbulent boundary layer calculation. For the sake of comparison between the methods he used three artificially developed wall shapes thought to be representative of the velocity profiles met in practice. The flow model C shown in Fig. 2. was used in an application of the Truckenbrodt's method computer program to compare the results with those obtained by Smith on an electric desk machine. The agreement between both results may be seen from Fig. 3.

Fig. 2 shows also the distribution of the momentum thickness obtained with the proposed flow model C. Three values of the shape parameter H at transition were assumed for an investigation of the effect of H_t on the position of turbulent separation. It can be seen that it has a slight effect.

A value of $R_\theta = 500$ was used for transition in accordance with Preston's suggestion that the Reynolds number for turbulent flow should not be less than 320.

4.2. Practical Applications of the New Analysis

The utility of the derived and computerised new analysis for predicting the development of turbulent boundary layers has been checked on several experimental boundary layers reported in the literature. The experiments which would test the accuracy and versatility of the new analysis must be of quite a general nature with respect to the external pressure gradient. Lewkowicz and Horlock (7) have applied the new analysis to the following known experiments.

(i) v. Doenhoff and Tetervin (1943) -(3)
(ii) Schubauer and Klebanoff (1950) -(17)
(iii) Newman (1953) -(10)
(iv) Bradshaw and Ferriss (1965) -(22)

The corresponding results show that the new analysis predicts the development of boundary layers as observed by Schubauer and Klebanoff and by Bradshaw and Ferriss quite well and its agreement with the experiments of Newman and of v. Doenhoff and Tetervin is almost as good. Two of the above experiments, namely those by Schubauer and Klebanoff and by Bradshaw and Ferriss, can be classified as classic experiments on turbulent boundary layer with adverse pressure gradients. This is mainly due to the comparitively high degree of accuracy of the actual measurements, large scale of the created boundary layers, turbulent quantities being measured as well as the distribution of mean velocities, accurate determination

of the skin friction coefficients. It is particularly important to know exactly the distribution of the external pressure gradient since the new analysis is sensitive to it.

In the present report only results with respect to the first two experiments are quoted and for the remaining two cases reference is made to Lewkowicz and Horlock (7).

For each of those experiments the external pressure gradient and the initial conditions are calculated from the reported observations. The initial conditions are carefully chosen; they should correspond to a stage of the boundary layer development where the boundary layer is fully turbulent.

Every test of the new analysis comprises at least three different boundary layer quantities being compared with the experimental observations. To make the test complete these must include:

(i) one of the skin friction coefficients (c_f or ω),
(ii) one of the boundary layer thicknesses (δ , δ^*, or θ)
(iii) either one of the mean velocities shape parameters (H or $\bar{H}$) or the free parameter Π .

This relative freedom of testing the new analysis is justified by the fact that all the quantities are obtained simultaneously in the result of the numerical solution, and that any sequence of the boundary layer quantities is uniquely convertible to the local variables ω , δ , and Π , and of course, vice versa.

4.2.1. Schubauer and Klebanoff's Experiment

The first comparison between experimental observations and theoretical prediction using the new analysis has been accomplished for the turbulent boundary layer developing under a strong adverse pressure gradient, generated by Schubauer and Klebanoff (17). The following results are plotted together with experimental points: shape parameter H (Fig. 4a), skin friction coefficient c_f. (Fig. 4b), boundary layer momentum thickness θ (Fig. 4c), absolute boundary layer thickness δ (Fig. 4d) and free parameter Π (Fig. 4e). In Fig. 4a the variation of the external pressure gradient is also shown. The agreement is seen to be reasonably good almost up to the point of separation which was determined experimentally to occur at $x = 25.4$ ft. The graphs displaying the variation H and θ with x (Fig. 4a and 4b) contain also these quantities obtained by Truckenbrodt's method (19). In the case of the shape parameter H the present method agrees well with the observations throughout 75% of the entire distance of development. Near separation the present method overestimates it whereas Truckenbrodt's method shows generally a slight trend to underestimation. The momentum thickness θ is in this region underestimated by both methods, although to a lesser

degree by the present method. The nearly impeccable prediction of the skin friction by the new analysis is noticeable (see Fig. 4b).

4.2.2. Bradshaw and Ferriss' Experiment

Bradshaw and Ferriss' rather unusual experiment (22) (where the turbulent boundary layer was brought to a state $H = 1.53$ and then, by weakening the external pressure gradient, reduced back to flat plate conditions, $U_\infty \propto x^a$ where $a = -0.255 \to 0$), displays an interesting test for any theoretical method of predicting the development of turbulent boundary layers.

The present new analysis predicts Bradshaw and Ferriss' boundary layer reasonably well, as shown in Figs. 5a, b and c. A very good agreement has been obtained for the momentum thickness growth θ, and the shape parameter H follows the experimental points, but the skin friction coefficient is slightly underestimated (by some 15%). However, Bradshaw and Ferriss indicated a possibility of slight three dimensionality in their experiment which could have affected the measurements of skin friction.

Bradshaw and Ferriss tested their experiment by calculating $\theta \cdot \frac{dH}{dx}$ from the observations as well as by using different analytical methods and presented the corresponding results as given by Fig. 6. On this diagram the curve $\theta \cdot dH/dx$ appropriate to the present method has been superimposed. It shows a substantial improvement in predicting Bradshaw's boundary layer.

5. Correction of Potential Flow for the Effect of Viscosity and Comparison with Experimental Results

5.1. Theoretical Considerations

In this paragraph an attempt is made to show the real value of considering viscous flow. This value lies not only in enabling the profile drag to be calculated and areas of separated flow to be avoided, but also in providing a condition for determining the cascade outlet angle and thus giving a unique pressure distribution.

Although the work described uses the hypothesis of Taylor (20) that as much positive as negative vorticity is discharged into the wake at the trailing edge, this is a simplifying idealisation which only applies to profiles which do not have excessive curvature near the trailing edge. Cases in which the hypothesis does not apply have been considered in (5).

The analysis given by Preston (12) was used to obtain the relationship:

$$(C_{pT})_S = (C_{pT})_P$$

This important relationship, which states that the static pressure coefficients on the blade surface must tend to the same value if the trailing edge is approached from either surface, gives the basis of a condition which will be used for obtaining unique, calculated pressure distributions.

The starting point for any cascade at a certain incidence is a series of pressure distributions for selected positions of rear stagnation point (e.g. Fig. 7). The initial task is therefore to select a unique pressure distribution (with corresponding outlet angle) on which to base subsequent boundary layer theory.

The first viscous approximation is applied by simply fairing in the pressure distributions to avoid severe velocity peaks at the trailing edge. This function is fulfilled in a real flow by means of the displacement effect of the boundary layer near to the trailing edge. It is recommended that the fairing in is achieved on both surfaces by extrapolating the pressure distribution tangentially from the 85% chord position. The 85% chord position is used as a result of a study of measured pressure distributions on blade profiles, since practically all of the pressure distributions examined indicated a linear change in pressure over the last 15% of chord. This conclusion agrees with that of Spence and Beasley (15) who worked on isolated aerofoils. The process is illustrated in Fig. 8.

The family of pressure distributions for a given inlet angle and a given range of outlet angles, having extrapolated portions for the last 15% of chord

length, is then examined for the static pressure difference in the trailing edge plane. The correctly determined pressure distribution is the one for which the difference in pressure coefficients at the trailing edge is zero.

The momentum thickness of each boundary layer at the trailing edge is required if a prediction of the profile drag is to be attempted; in addition the displacement thickness must be known if any attempt is to be made to perform an iterative scheme as a further correction for the displacement effect of the blade boundary layer /wake combination.

Methods available for computation of these boundary layer thicknesses have been described in paragraph 3. Calculations of the wake characteristics are described in (5).

The correction of the potential flow pressure distribution for profiles with a rounded trailing edge thus takes the form of an iterative procedure starting with a range of pressure distributions,using the first viscous approximation as a basis for calculating the boundary layers and wake and finally correcting for the displacement effect. The procedure is detailed in (5).

5.2. Theoretical Prediction for a Certain Compressor Cascade

The described theories were applied to a compressor cascade for which the potential flow could be calculated exactly using the analysis of (4). The profile, as shown in Fig. 9 is set at $\sigma = 36^{o}$ and $s/c = 0.875^{o}$. The potential flow was obtained at an incidence of $1^{o}50'$ for a range of rear stagnation point positions. All of the pressure distributions thus obtained were then extended from the 85% chord position and the difference between pressure coefficients in the trailing edge plane was plotted as a function of the position of rear stagnation point. The graph was interpolated to give $\Delta C_{pT} = 0$ and the potential flow calculations were re-run for the given position of rear stagnation point. The suction and pressure surface distributions thus obtained were extrapolated from $x/c = 0.85$ so that they touched at the trailing edge. This pressure distribution was the result of the first viscous approximation and satisfied the condition of zero nett vorticity discharge.

Although the first viscous approximation should be sufficiently accurate for profiles of low loading, an attempt was made to correct for the displacement effect of the calculated boundary layer and wake in order to discover if any advantage were to be gained by such an extension.

The calculation of the boundary layers was performed using the combined Thwaites-Truckenbrodt program with transition assumed to occur at the suction

peak and an initial value of H = 1.4 for the turbulent layer. The velocity distribution used was that obtained from the first viscous approximation. On the basis of the boundary layer conditions at the trailing edge, the wake was computed for one chord length downstream of the trailing edge. The locus of original profile plus boundary layer and wake displacement thicknesses thus gave a completely new profile, as seen in Fig. 11.

The Martensen (9) method potential flow computer program was then used to calculate potential flow around the new cascade for a small range of α_2 in the region of the previously determined value.

It was found that the velocities were not constant along the wake but increased rapidly towards the station one chord downstream. This is shown in Fig. 12 which gives both first and second viscous approximations.

Ideally a further iteration would have been effected by calculating boundary layer and wake thicknesses for the new pressure distribution and hence re-calculating the potential flow around the slightly altered profile. Due to the inconsistency of results of the second viscous approximation a further iteration was not carried out.

Since the inconsistency obviously arose in the addition of the wake displacement thickness and attempted calculation of potential flow around the complicated new shape, this source of error was removed. The locus of profile and displacement thickness was rounded off in the trailing edge plane. The potential flow was then calculated around this new profile. The result, which is also shown in Fig. 12 revealed that the velocity distribution had converged to one very little different from that of the first viscous approximation.

5.3. Experiments on the Above Cascade

Accurate experimental results were required for the flow around the cascade of analytically derived profiles.

The experiments were performed on the Liverpool University No. 1 low speed cascade tunnel which has provision for porous side wall boundary layer bleed in addition to the usual slot suction facilities. The cascade consisted of 9 blades of 6" chord and 12" span at the fixed inlet angle of 52°50'. On the centre blade 34 pressure tappings were provided for measuring the static pressure distribution. All tests were carried out at Re = 1.95×10^5 with a free stream turbulence level of 0.45%; side wall suction was adjusted to give an axial velocity ratio of unity.

Traversing facilities included claw probes, for measuring yaw angle and total pressure at inlet and outlet. Fourteen static pressure tappings were also provided upstream of the cascade. Traversing for yaw angle, total and static

pressures was also possible in any direction using a wedge yawmeter.

For measuring the profile boundary layers a 0.032" o.d. pitot tube was manufactured. The tube was traversed relative to the blade surface by the arrangement shown in Fig. 10. A. 6.B.A. brass study was drilled centrally to receive the pitot tube to which it was soldered. The plastic pressure tubing was fitted directly over the study and the whole was mounted within a threaded collar which was finished flush with the blade. Thus by rotating the pitot through 360^{o} it was possible to traverse the tube by a previously determined increment.

Initial testing was carried out within turbu ence generators or transition devices. The quantities Re, α_1, α_2 and axial velocity ratio were obtained from integration of claw yawmeter traverses in conjunction with appropriate static pressure measurements. Each traverse contained 60 pitchwise positions.

Blade surface boundary layer traverses were made at three stations on the suction surface and one on the pressure surface. Corresponding to the boundary layer traverses a blade pressure distribution was obtained. The reading of a Preston tube was also taken for each measuring station enabling results to be plotted on a U/u_τ vs. $\log_{10}\left(\frac{u_\tau y}{\nu}\right)$ graph. A sizeable wake component was evident in such a plot. Fig. 15 shows the results of the traverses corresponding to the pressure distribution given in Fig. 13. The displacement and momentum thicknesses of boundary layers and wake were subsequently obtained and are presented in Fig. 18. The Young and Maas correction (21) was applied to all boundary layer results.

Although useful results were obtained without the use of artificial means of profile boundary layer control the existence of a laminar separation bubble made comparison with theoretical results impossible. The laminar separation was therefore eliminated by causing early transition using a 3.1/2" mesh turbulence grid and alternatively isolated 0.013" diameter roughness spheres on the profile leading edge. No boundary layer traverses were taken with the turbulence grid in position, but the pressure distribution is shown in Fig. 13.

The first application of roughness spheres was too liberal and, although the laminar separation bubble was eliminated, a region of trailing edge turbulent separation was present. The effect of this is evident in the pressure distribution of Fig. 14, and was confirmed by use of lamp-black and paraffin flow visualisation. Upon removal of some roughness the desired state of unseparated flow was attained.

A comparison of boundary layer profiles for blades with and without leading edge roughness under similar inlet conditions is given in Fig. 16. It will be seen that the boundary layer with early transition is nearer to separation at this station of $x / c = 0.855$. This was further confirmed when

results were plotted on a U/u_τ vs. $\log_{10}\left(\frac{u_\tau y}{\nu}\right)$ graph.

Results are given in Fig. 17 for various suction surface chordwise stations when early transition was precipitated. Once more results, which were obtained at .A.V.R. = 1, were repeatable and showed little scatter. The corresponding pressure distribution (Fig. 14) is the one which is compared with theoretical results in the next paragraph.

For further details concerning experimental apparatus, technique and quality of flow the reader should consult (6).

5.4. Comparison between Theory and Experiment

It was evident that, since the results of the second viscous approximation on the profile plus wake indicated velocities which rose sharply towards the end of the wake, these results were not reliable. The results obtained by rounding off the displacement thickness in the trailing edge plane were much more reliable and did not diverge from the first viscous approximation. Because of this, recourse was made to the results of the first viscous approximation - the 'faired in' potential flow was a correctly applied condition for unique determination of the circulation. The velocity distribution for this (the full line in Fig. 12) was therefore used, with its associated outlet angle, as a basis for the comparison of theoretical and experimental results. The computed boundary layer thicknesses, based upon this velocity distribution, were also used in a comparison with experimentally measured thicknesses.

The outlet angle results, measured experimentally over two pitches at one chord downstream of the trailing edge and calculated theoretically an infinite distance downstream, were respectively $31^{\circ}03'$ and $31^{\circ}34'$ giving an error of just over 30'.

Agreement between pressure distributions was also noteworthy and the two pressure distributions are given in Fig. 19. Apart from a very slight discrepancy near the suction peak the two curves coincide, no scatter being present in either distribution. The maximum difference between theoretical and experimental pressure coefficients is 1% of the maximum difference between stagnation and suction peak values of C_p.

Boundary layer results were also compared and Figs. 20 and 21 reveal the agreement between theory and experiment.

The results for the suction surface displacement thickness indicate a maximum

difference of 6% of the maximum value of δ^*/c between theory and experiment, with close agreement in the trailing edge region.

Although the displacement thickness for the one point on the pressure surface is in very close agreement with the theoretical prediction at that point, some doubt must be entertained since the wake measurement taken within 0.010" of the trailing edge, shows far higher values of displacement thickness. The reason for this is probably the effect of the thickness of the trailing edge which will have affected the wake measurements.

Comparison of momentum thicknesses, as shown in Fig. 21, gives reasonable agreement between theory and experiment. A maximum error in θ/c of 22% is present on the suction surface and the pressure surface comparison shows much closer agreement for momentum thickness than for displacement thickness.

6. Conclusions

Since the main emphasis was on the use of the boundary layer calculation in high speed computer programs, a general program was evolved using the Thwaites' and Truckenbrodt's theories for a wide range of assumptions concerning initial and transition conditions. The program gives good agreement with the results of Smith, who calculated the turbulent layer for a chosen flow model.

The agreement between the new analysis of Lewkowicz and Horlock and the experimental boundary layers on which it was tested is good for the experiments by Schubauer and Klebanoff and by Bradshaw and Ferriss. In the case of Schubauer and Klebanoff's experiment, the new analysis gives better agreement than the method of Truckenbrodt.

For Bradshaw and Ferriss' experiment indicates better agreement than the methods of Maskell, Spence, von Koenhoff and Tetervin and Head. However, some considerable difference between $\theta \cdot dH/dx$, predicted by the new analysis and that measured by Bradshaw and Ferriss is still evident.

The main shortcomings of the new analysis are as follows:-

The new analysis does not provide a definite criterion for the separation of two dimensional turbulent boundary layers, extrapolation of the c_f curves to zero being the only indication of separation. The distribution of the free stream velocity U_∞ is fed into the analysis in the form of the external pressure gradient $(2/U_\infty) \cdot (d U_\infty/dx)$, necessitating the use of either graphical differentiation or polynomial curve fitting.

The difficulty in the calculation of the flow around aerofoils with rounded trailing edges is overcome by the application of viscous flow theory. A new unique condition is found using the empirical 'fairing-in' of Spence and the hypothesis of 'zero nett vorticity discharge'. The methods of boundary layer calculation can be used for the pressure distribution thus obtained in order to predict the loss and separation characteristics of the cascade and also to correct iteratively for the displacement effect of boundary layer and wake.

Calculations are performed on a cascade for which the potential flow is known exactly. It is found that although the theoretical addition of boundary layer displacement thickness succeeds, the consideration of the wake is not successful. It is concluded that for medium incidence the results obtained by using the first viscous approximation and the condition of zero nett discharge of vorticity render further consideration of viscosity unnecessary.

A cascade of analytically derived profiles was tested experimentally and the

results of blade surface boundary layer traverses are presented in addition to angle traverses and pressure distributions. One experiment, in which a transition device was used, is selected for comparison with theoretical results.

A comparison between the pressure distributions of the chosen test and the theoretically obtained first viscous approximation gives excellent agreement.

It is finally concluded, that, the cascade pressure distributions, outlet angles and all boundary layer parameters, can be fairly accurately predicted for the usual two-dimensional, incompressible cascade flows.

ACKNOWLEDGEMENTS

The authors wish to thank Professor J.H. Horlock for instigating the report and for his encouragement throughout. They are also indebted to Bristol Siddeley Engines Ltd., for giving permission to use their computer program of Martensen's method of potential flow analysis.

REFERENCES

1. Clauser, F.H. — Turbulent boundary layer in adverse pressure gradients. J. Aero. Sci. 21, Vol. 21, pp. 91-108.

2. Coles, D. — The law of the wake in the turbulent boundary layer. J. Fluid Mech. Vol. I, pp. 191-226.

3. v. Doenhoff, A.E. & Tetervin, N. — Determination of general relations for the behaviour of turbulent boundary layers. N.A.C.A. Rep. 772. (1943).

4. Gostelow, J.P. — Potential flow through cascades, a comparison between exact and approximate solutions. A.R.C. C.P.807 (1964).

5. Gostelow, J.P. — The calculation of incompressible flow through cascades of highly cambered blades. U.L.M.E./B.9. (1965).

6. Gostelow, J.P. — The accurate prediction of cascade performance. Dissertation, Liverpool University. (Sept. 1965).

7. Lewkowicz, A.K. & Horlock, J.H. — An implicit approach to calculation of two dimensional turbulent boundary layers. U.L.M.E./B.19 (1965).

8. Ludweig, H. & Tillmann, W. — Investigations of the wall shearing stress in turbulent boundary layers. N.A.C.A. TM 1285, (May 1950).

9. Martensen, E. — Calculation of pressure distribution over profiles in cascade in two dimensional flow by means of a Fredholm Integral Equation. Arch. Rat. Mech. and Analysis. Vol. No. 3 (1959).

10. Newman, B.G. — Some contributions to the study of turbulent boundary layers near separation. Austr. Dept. Supply. Rep. ACA 53, (1951).

11. Pinkerton, R.M. — Calculated and measured pressure distributions over the midspan section of a N.A.C.A. 4412 airfoil. N.A.C.A. TR 563 (1936).

12. Preston, J.H. — The calculation of lift taking account of the boundary layer. A.R.C. R & M 2725 (November 1949).

13. Schlichting, H. — Berechnung der reibungslasen inkompressiblen strömung für ein vorgegebener ebenes schaufelgitter. V.D.I. Forschungsheft 447 (1955).

14. Speidel, L. & Scholz, N. — Untersuchungen über die Strömungsverluste in ebenen Schanfelgittern. V.D.I. Forschungsheft 464 (1957).

15. Spence, D.A. & Beasley, J.A. — The calculation of lift slopes allowing for boundary layer with application to the R.A.E. 101 and 104 aerofoils. A.R.C. R & M 3137 (February 1960).

16. Smith, D.J.L. — Turbulent boundary layer theory and its application to blade profile design. A.R.C. CP 868 March 1965.

17. Schubauer, G.B. & Klebanoff, P.S. — Investigation of separation of the turbulent boundary layer. N.A.C.A. TN 2133. (1950).

18. Thwaites, B. — Approximate calculation of the laminar boundary layer. Aeronaut. Q. Vol. I pp 245-280. (1949).

19. Truckenbrodt, E. — A method of quadrature for calculation of the laminar and turbulent boundary layer in the case of plane and rotationally symmetrical flow. N.A.C.A. TM 1379. May 1955.

20. Taylor, G.I. — Note on the connection between the lift on an aerofoil in a wind and the circulation around it. Phil. Trans. R. Soc. A. Vol. CCXXV (1925) pp. 238-245.

21. Young, A.D. & Maas, J.N. — The behaviour of a pitot tube in a transverse of total pressure gradient. A.R.C. R & M 1770 September 1936.

22. Bradshaw, P. & Ferriss, D.H. — The response of a retarded equilibrium turbulent boundary layer to the sudden removal of pressure gradient. N.P.L. Aero. Rep. 1145, (1965).

D77010/1/125875 K4 12/66 CL & XL

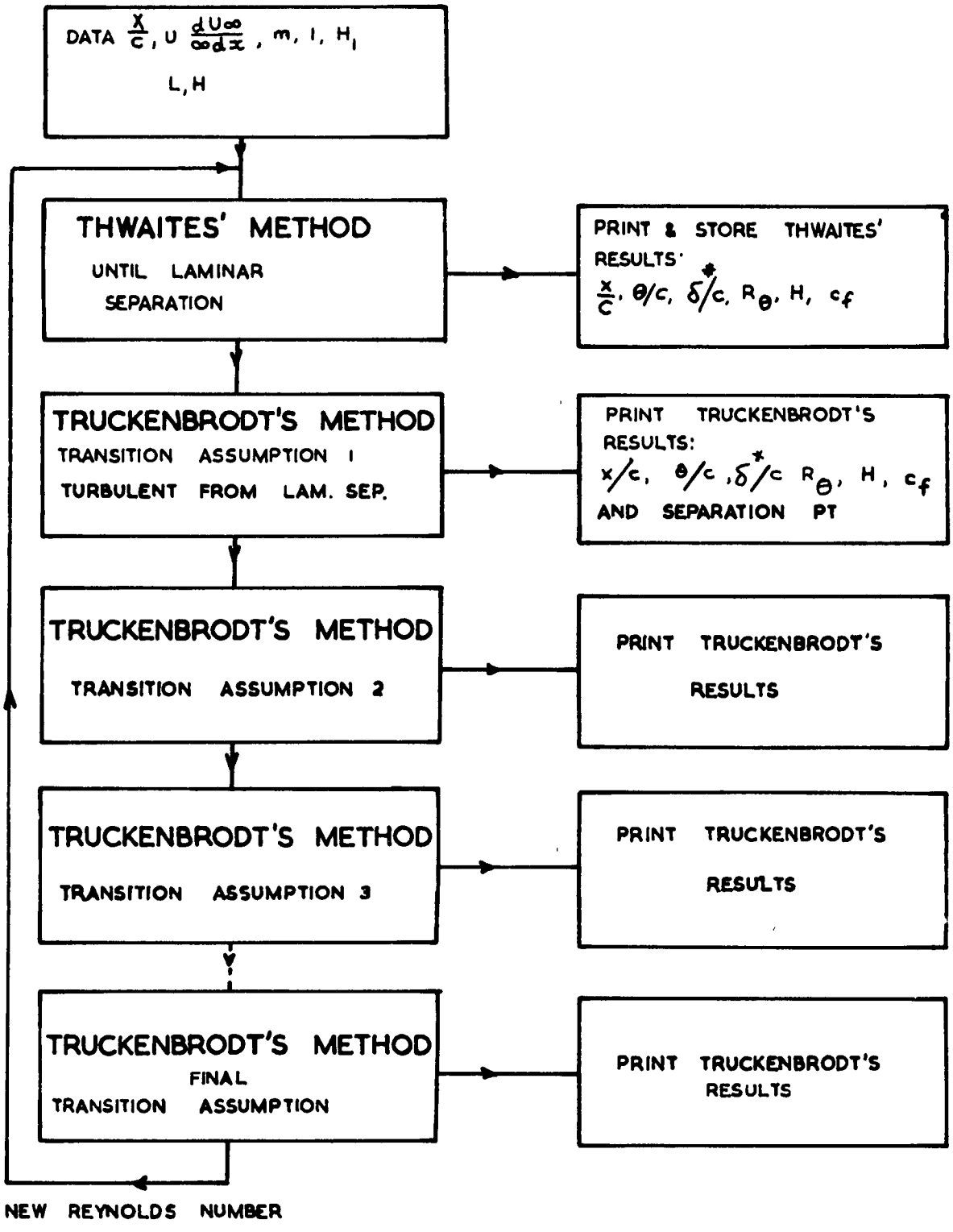

FIG. 1a FLOW DIAGRAM OF THWAITES – TRUCKENBRODT COMPUTER PROGRAM.

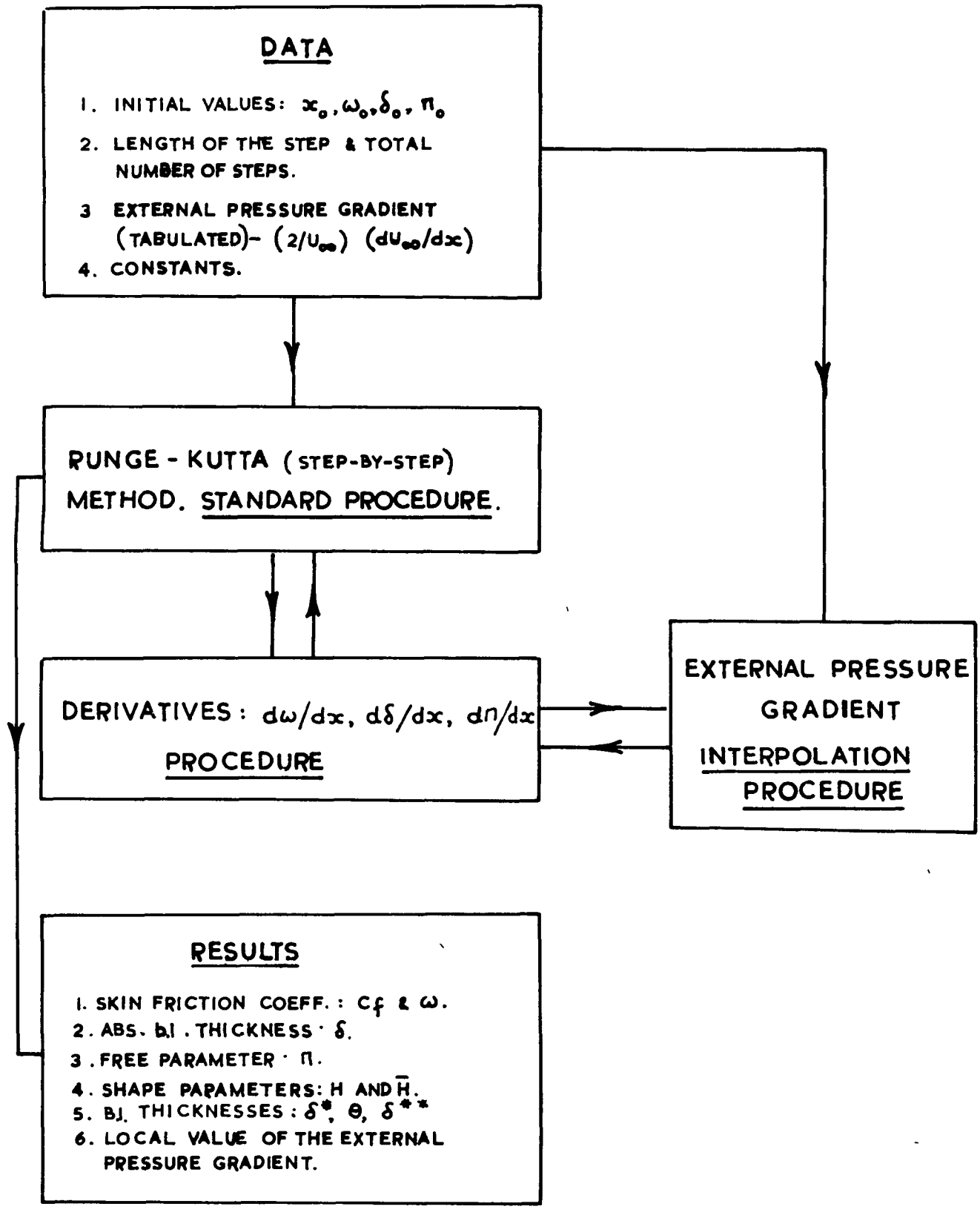

FIG. 1b FLOW DIAGRAM OF THE COMPUTER PROGRAM PERTINENT TO THE NEW ANALYSIS.

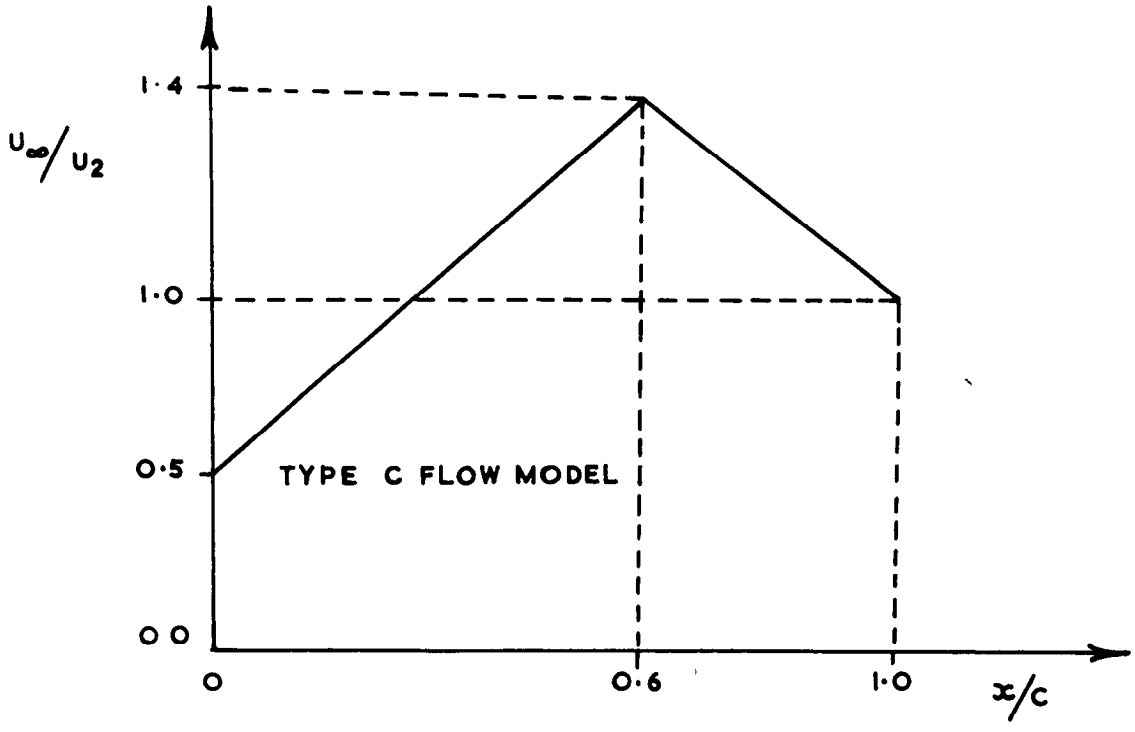

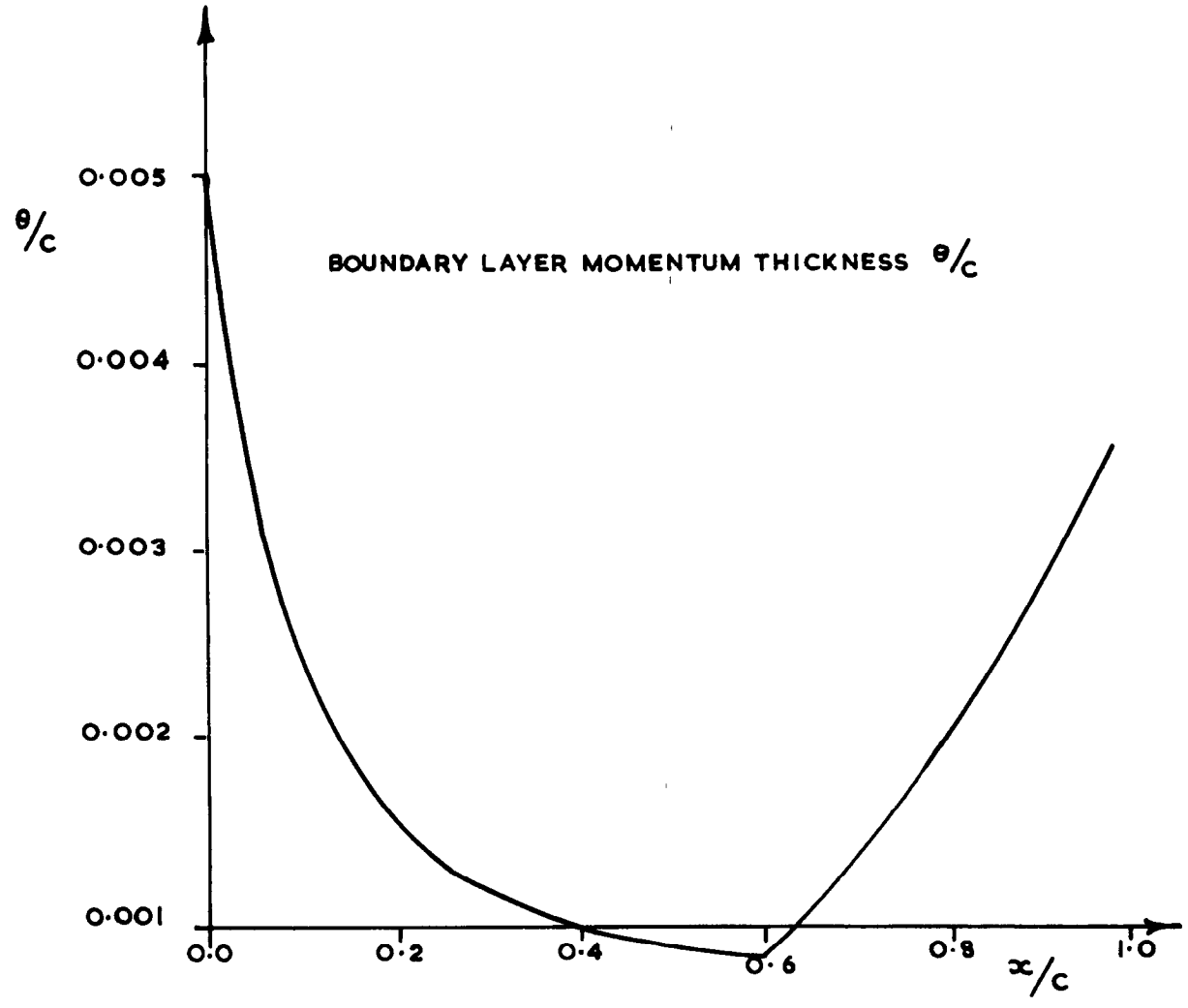

FIG.2 TYPE C FLOW MODEL [SMITH (16)] AND COMPUTER PROGRAM RESULT FOR MOMENTUM THICKNESS DISTRIBUTION

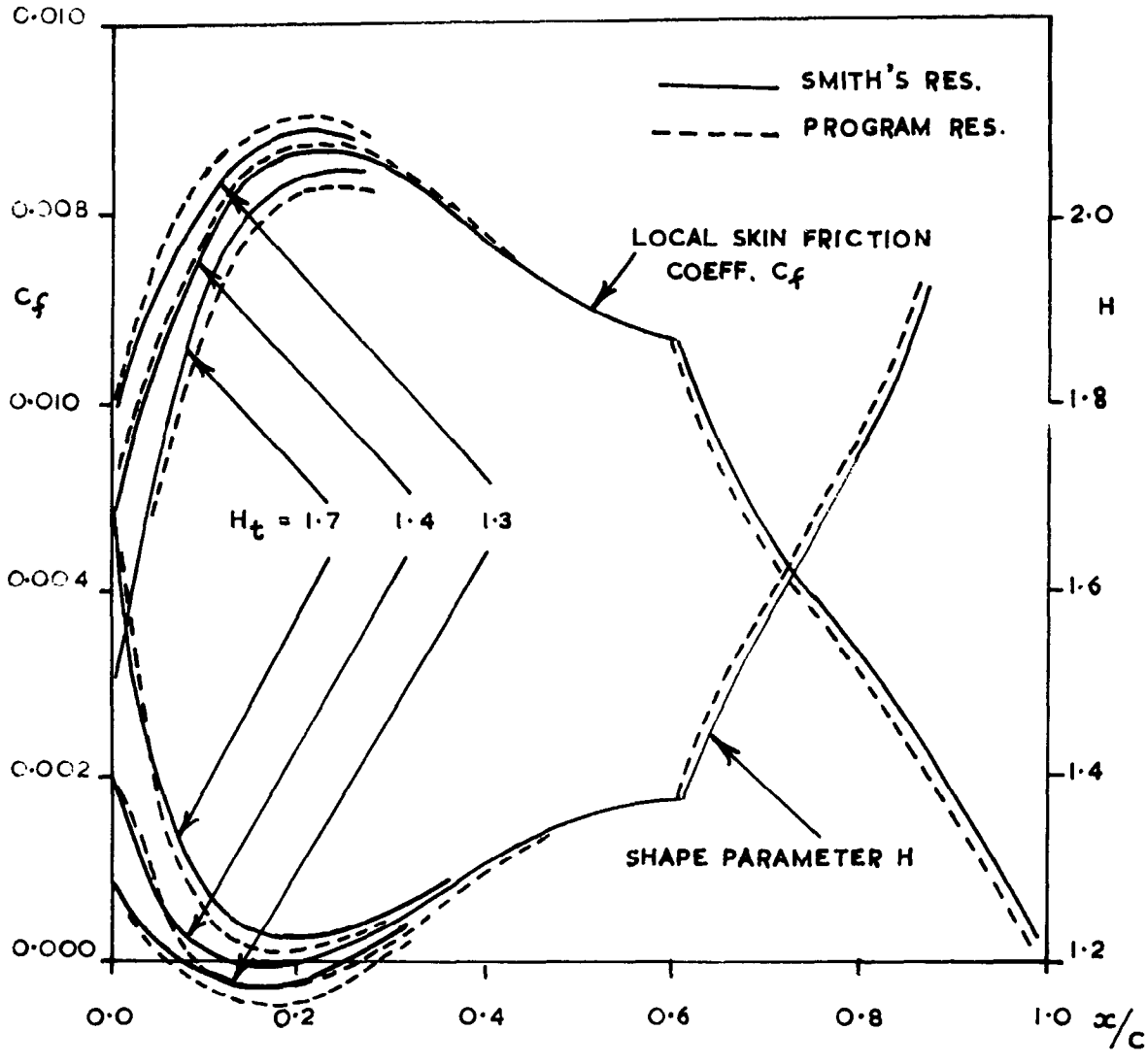

FIG. 3 TURBULENT BOUNDARY LAYER PREDICTED BY TRUCKENBRODT'S METHOD

COMPARISON BETWEEN THE COMPUTER PROGRAM AND SMITH'S CALCULATION.

(TYPE C FLOW MODEL)

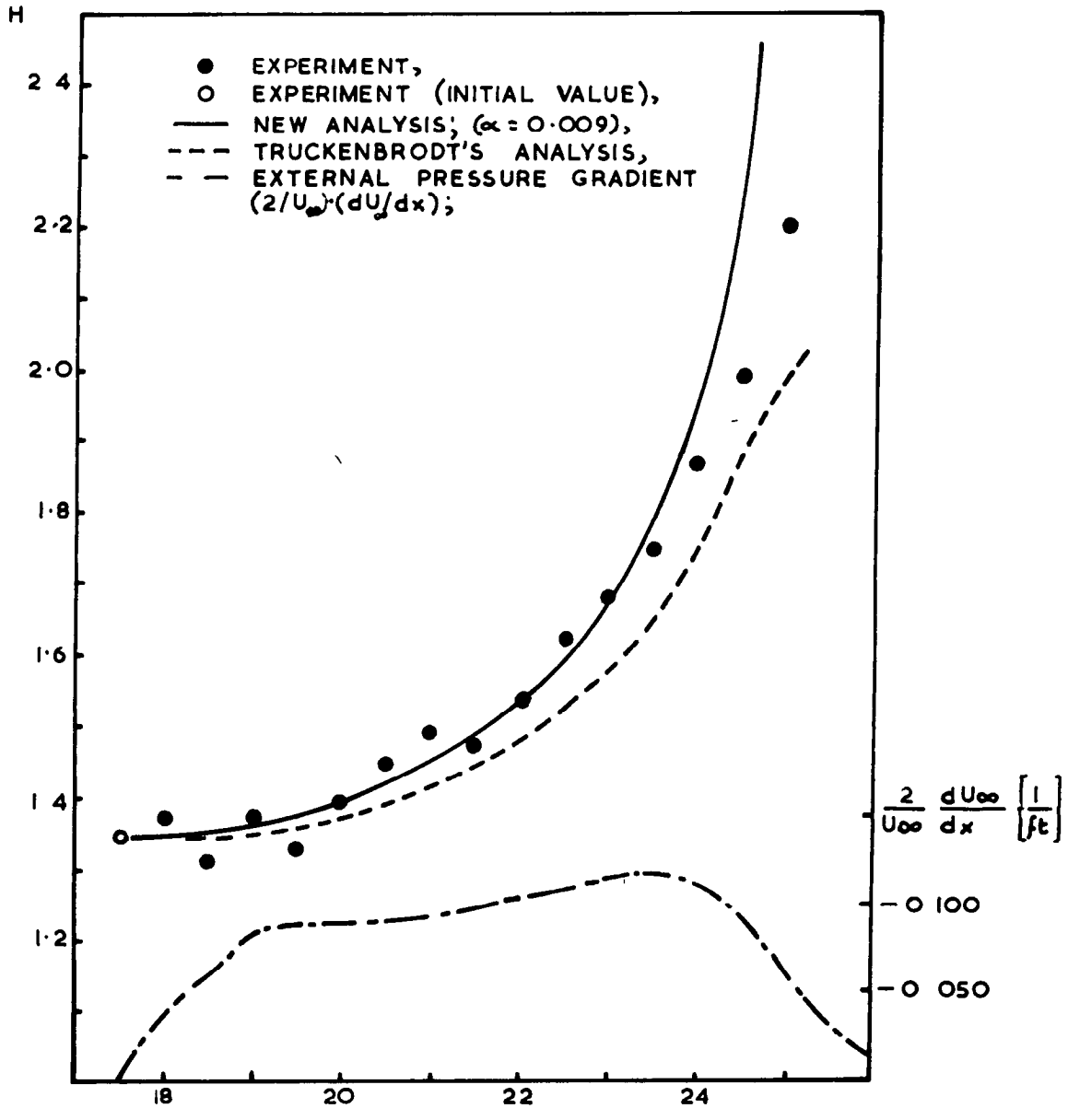

FIG. 4a SHAPE PARAMETER H. EXPERIMENT DUE TO SCHUBAUER AND KLEBANOFF [17] ALSO EXTERNAL PRESSURE GRADIENT $(2/U_\infty)\cdot(dU_\infty/dx)$.

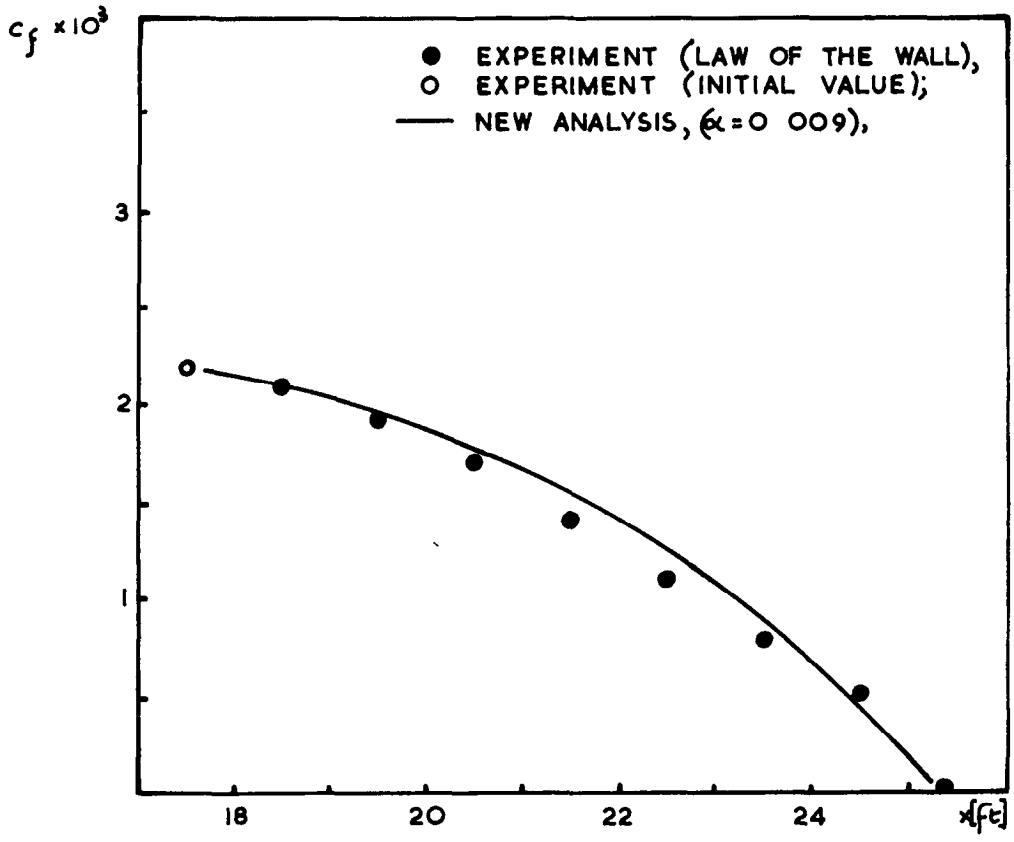

FIG. 4b SKIN FRICTION COEFFICIENT c_f.
EXPERIMENT DUE TO SCHUBAUER AND KLEBANOFF [17]

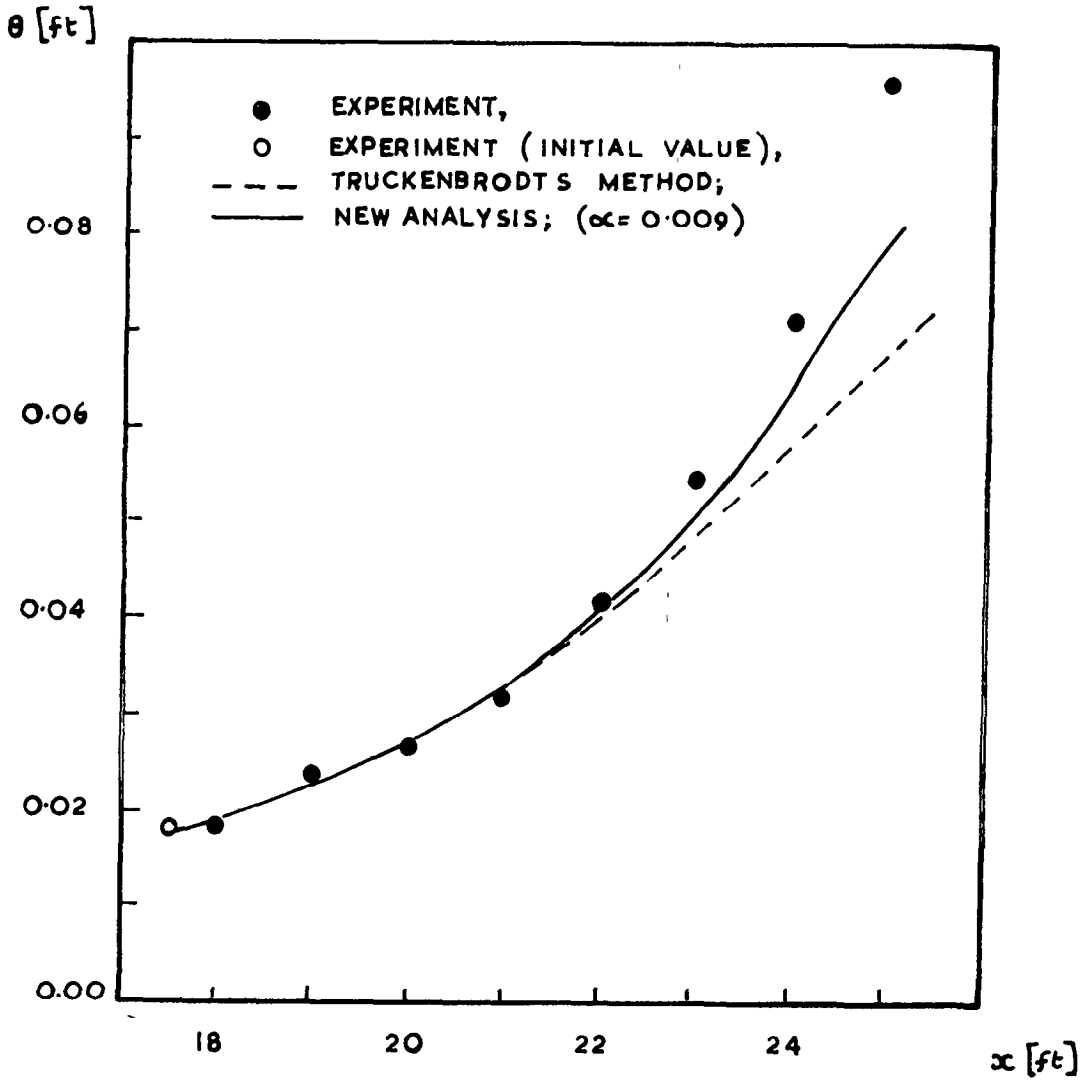

FIG.4c BOUNDARY LAYER MOMENTUM THICKNESS θ.

EXPERIMENT DUE TO SCHUBAUR AND KLEBANOFF (17)

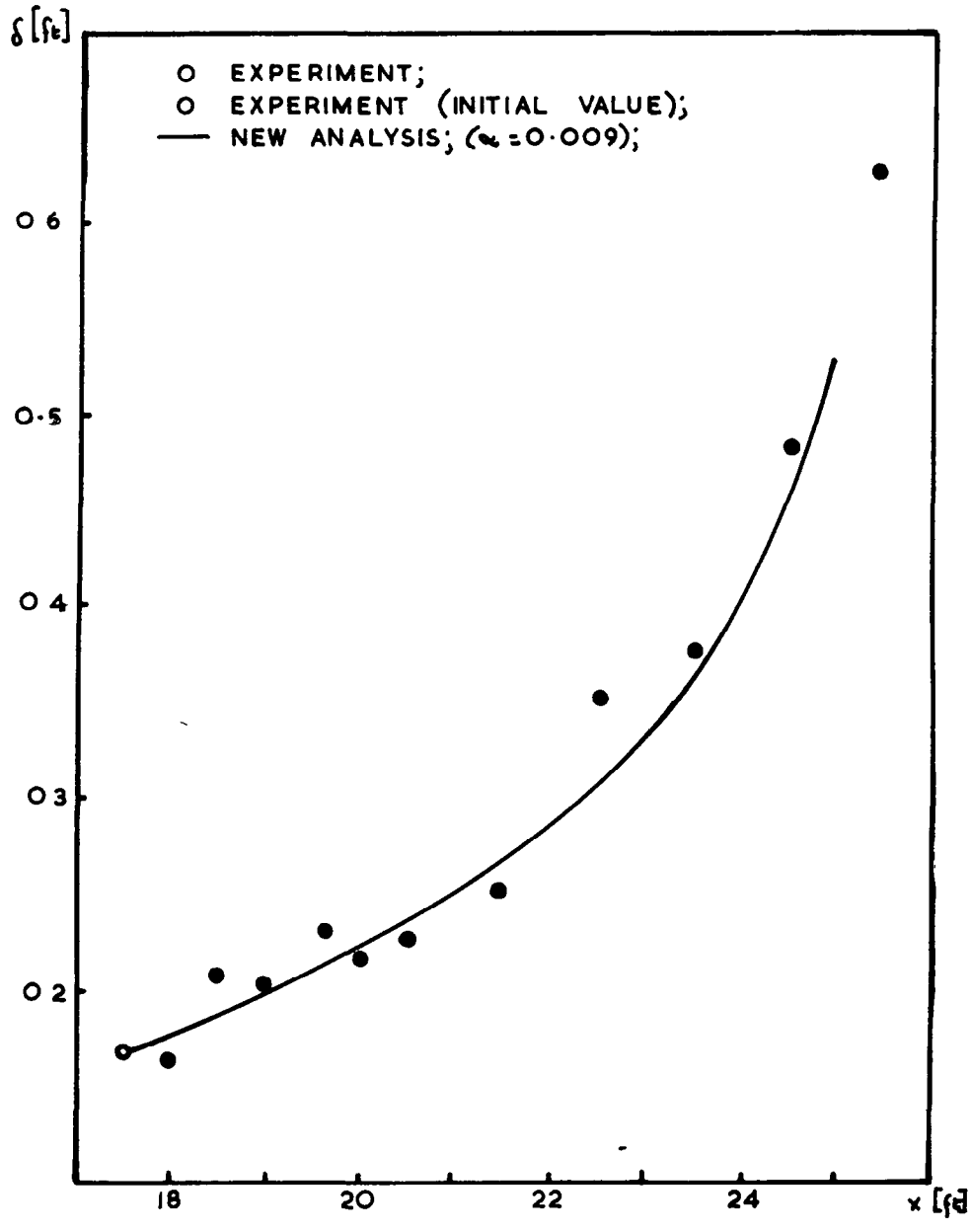

FIG. 4 d. ABSOLUTE BOUNDARY LAYER THICKNESS δ.
EXPERIMENT DUE TO SCHUBAUER AND KLEBANOFF [17]

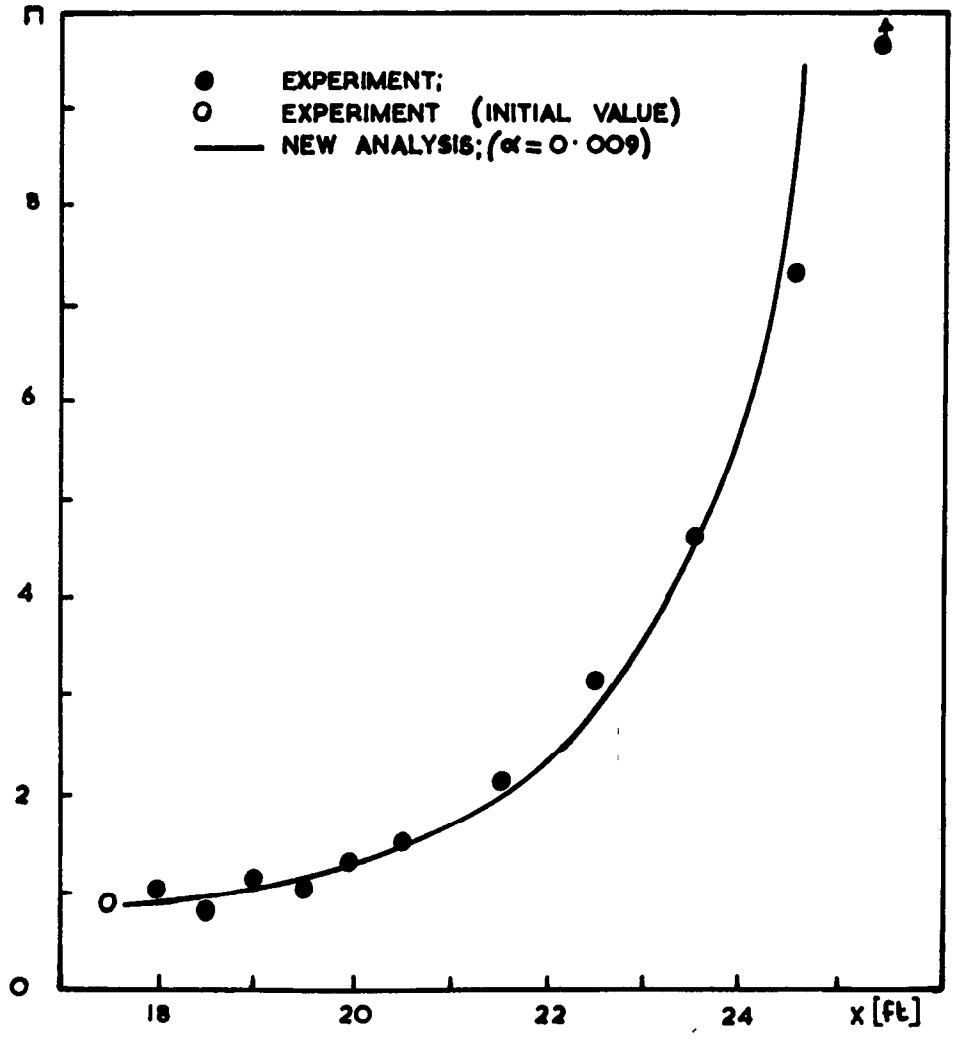

FIG. 4c FREE PARAMETER Π;
EXPERIMENT DUE TO SCHUBAUER AND KLEBANOFF [17]

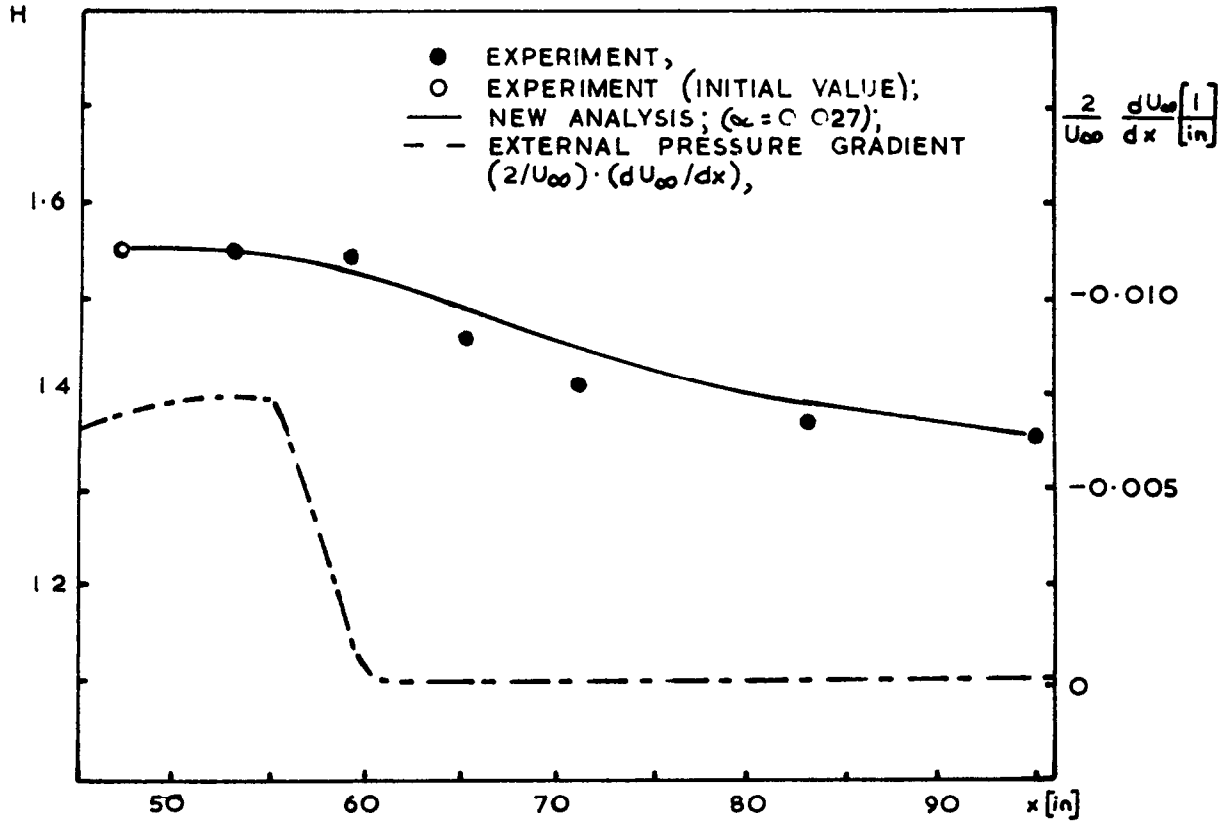

FIG. 5a SHAPE PARAMETER H. EXPERIMENT DUE TO BRADSHAW AND FERRISS [22] ($\alpha = -0.255 \rightarrow 0$) ALSO EXTERNAL PRESSURE GRADIENT $(2/U_\infty)\cdot(dU_\infty/dx)$.

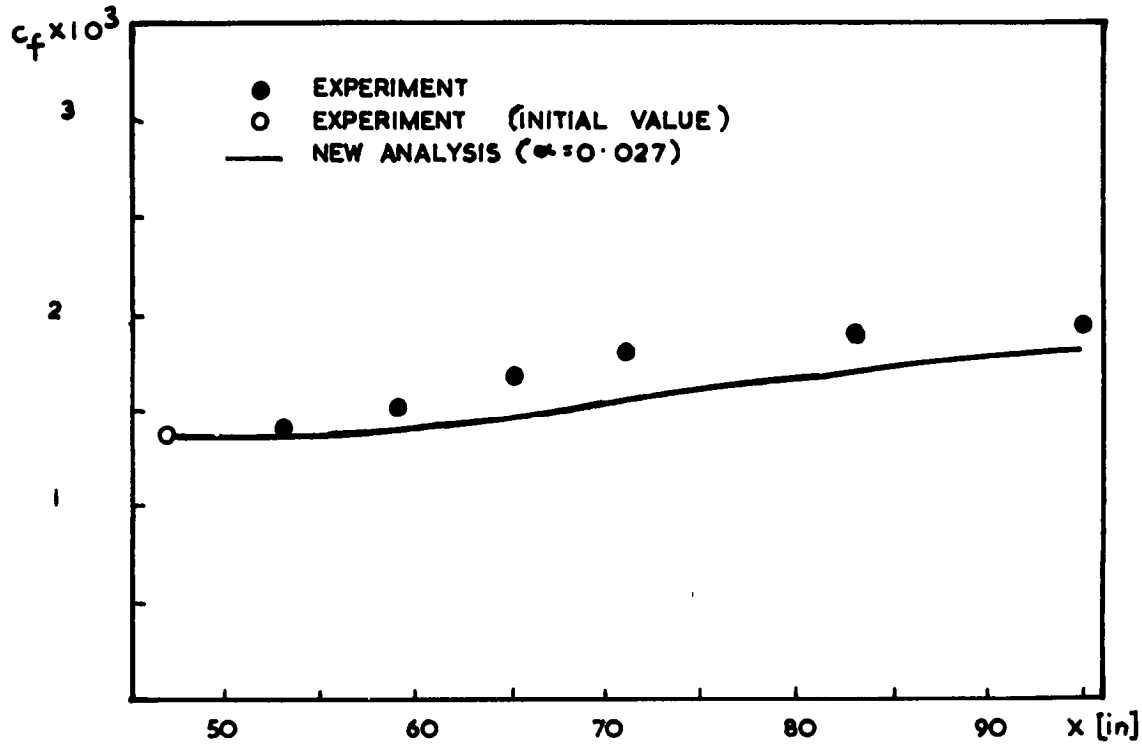

FIG. 5b SKIN FRICTION COEFFICIENT c_f

EXPERIMENT DUE TO BRADSHAW AND FERRISS [22]
($a = -0.255 \rightarrow 0$)

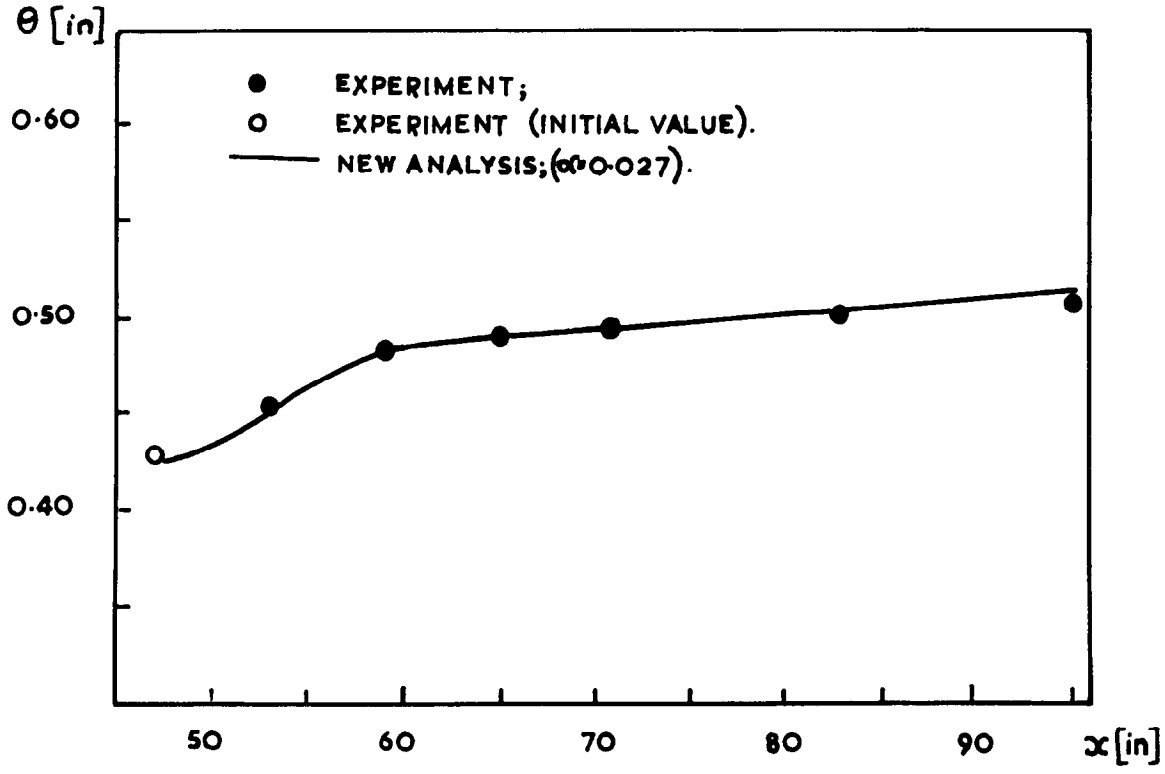

FIG. 5c BOUNDARY LAYER MOMENTUM THICKNESS θ.
EXPERIMENT DUE TO BRADSHAW AND FERRISS (22)
(a = -0·255 → 0)

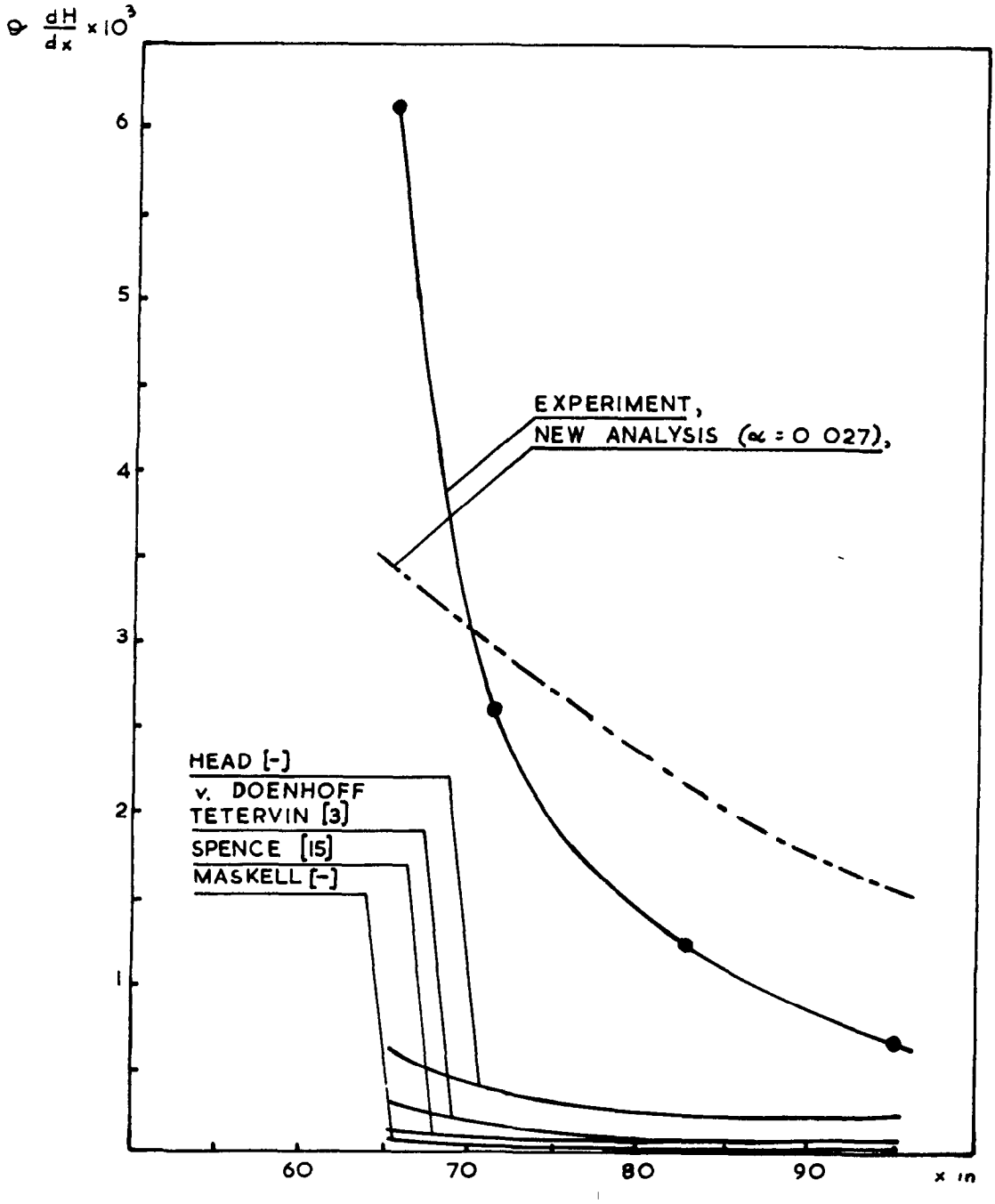

FIG. 6 EXPERIMENTAL θ (dH/dx) DUE TO BRADSHAW AND FERRISS ($a = -0{\cdot}255 \rightarrow 0$) COMPARED WITH RESULTS OBTAINED FROM DIFFERENT ANALYSES OF DEVELOPMENT OF TURBULENT B. LAYER. (ALL CURVES, EXCLUDING NEW ANALYSIS, AFTER BRADSHAW AND FERRISS [22])

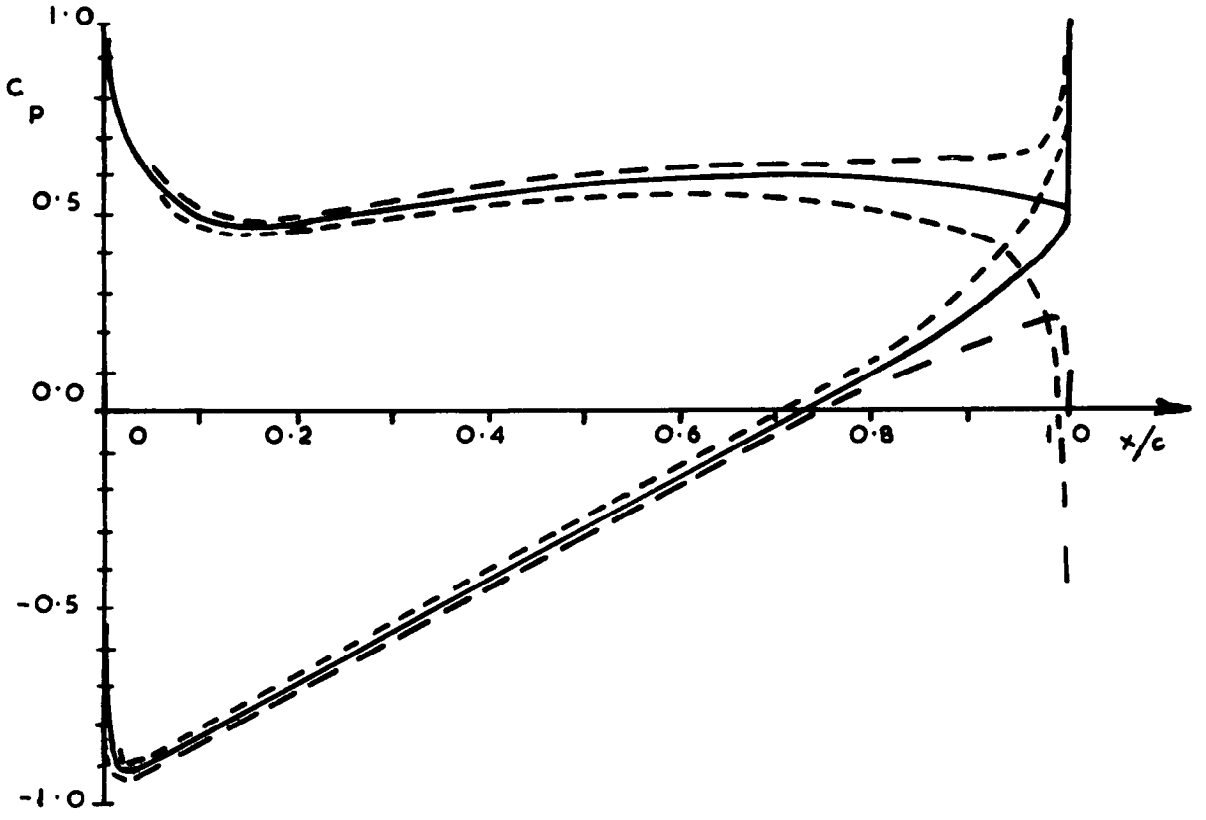

FIG. 7 EFFECT OF LOCATION OF REAR STAGNATION POINT ON PRESSURE DISTRIBUTION FOR ANALYTICAL PROFILE WITH S/C = 1·15

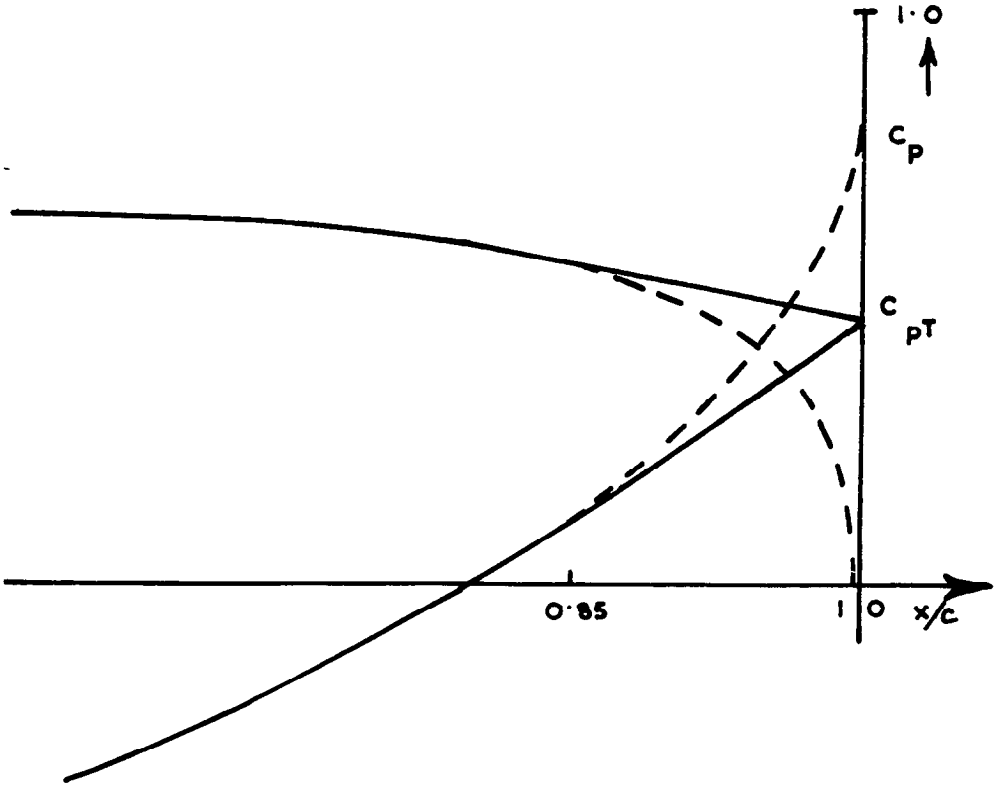

FIG. 8 ILLUSTRATION OF 'FAIRING IN' PROCESS

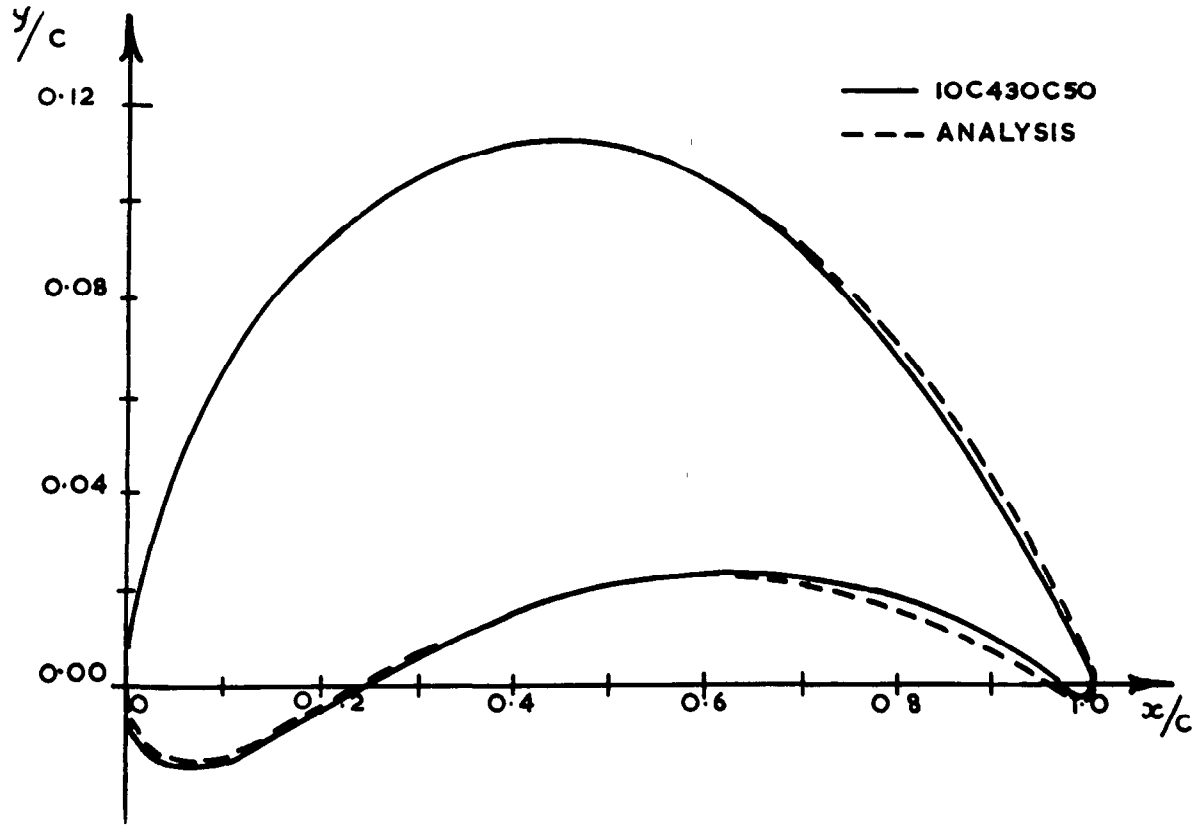

FIG.9 COMPARISON BETWEEN STANDARD C4 AND ANALYTICAL PROFILE

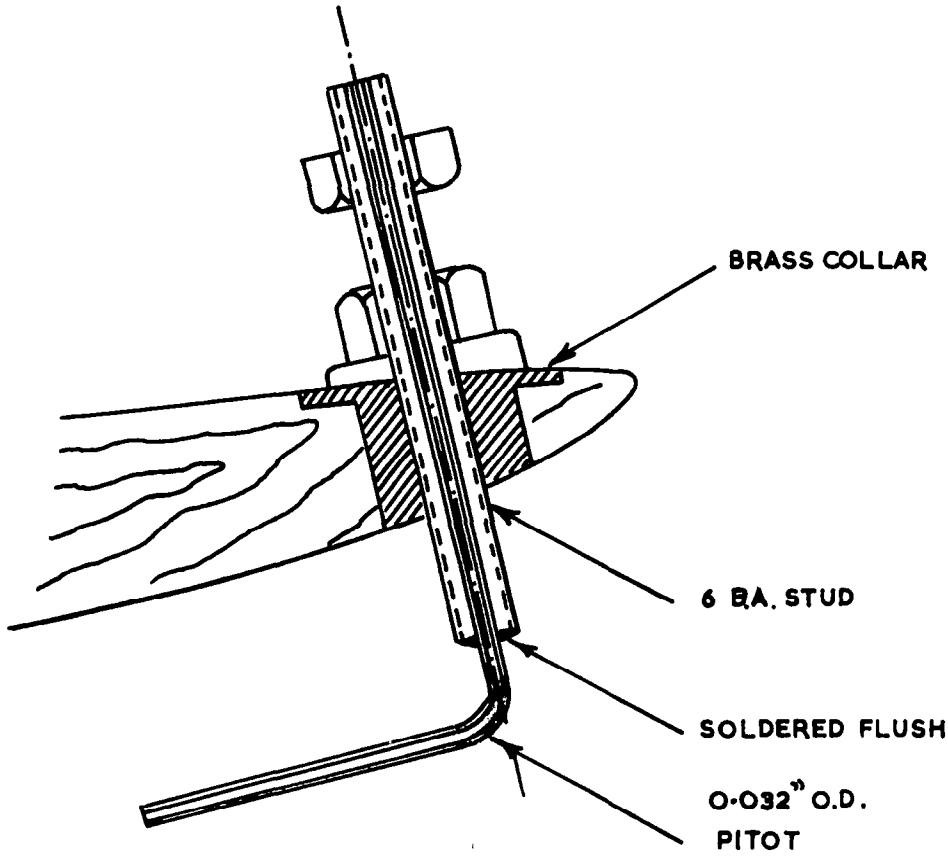

FIG.10 PROFILE BOUNDARY LAYER PROBE

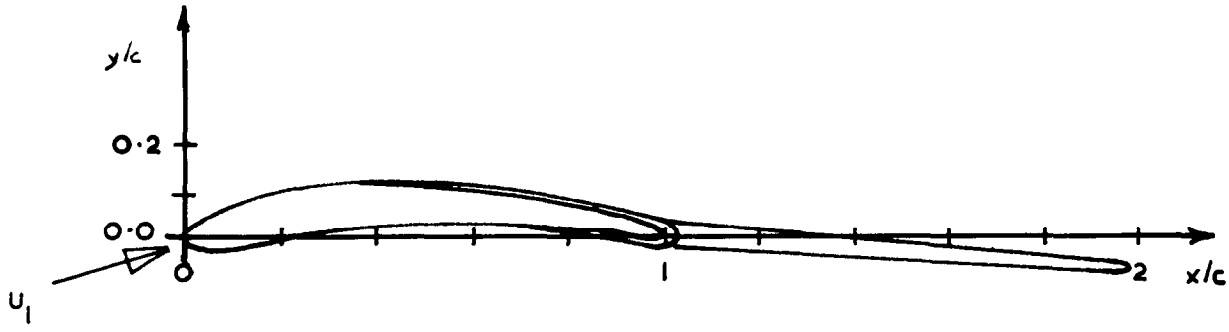

FIG. 11 PROFILE PLUS DISPLACEMENT THICKNESS

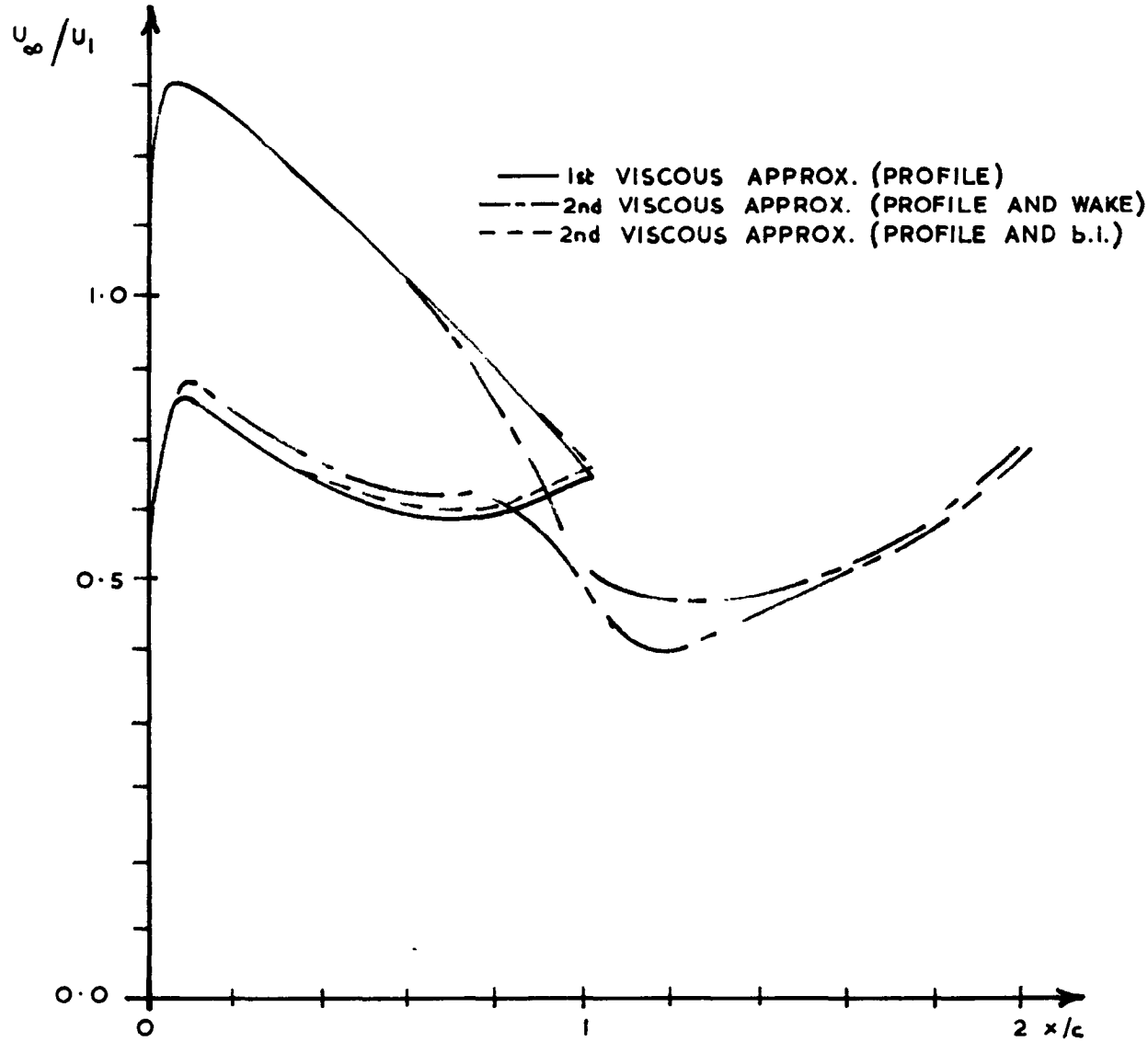

FIG. 12 VELOCITY DISTRIBUTIONS ON PROFILE AND WAKE

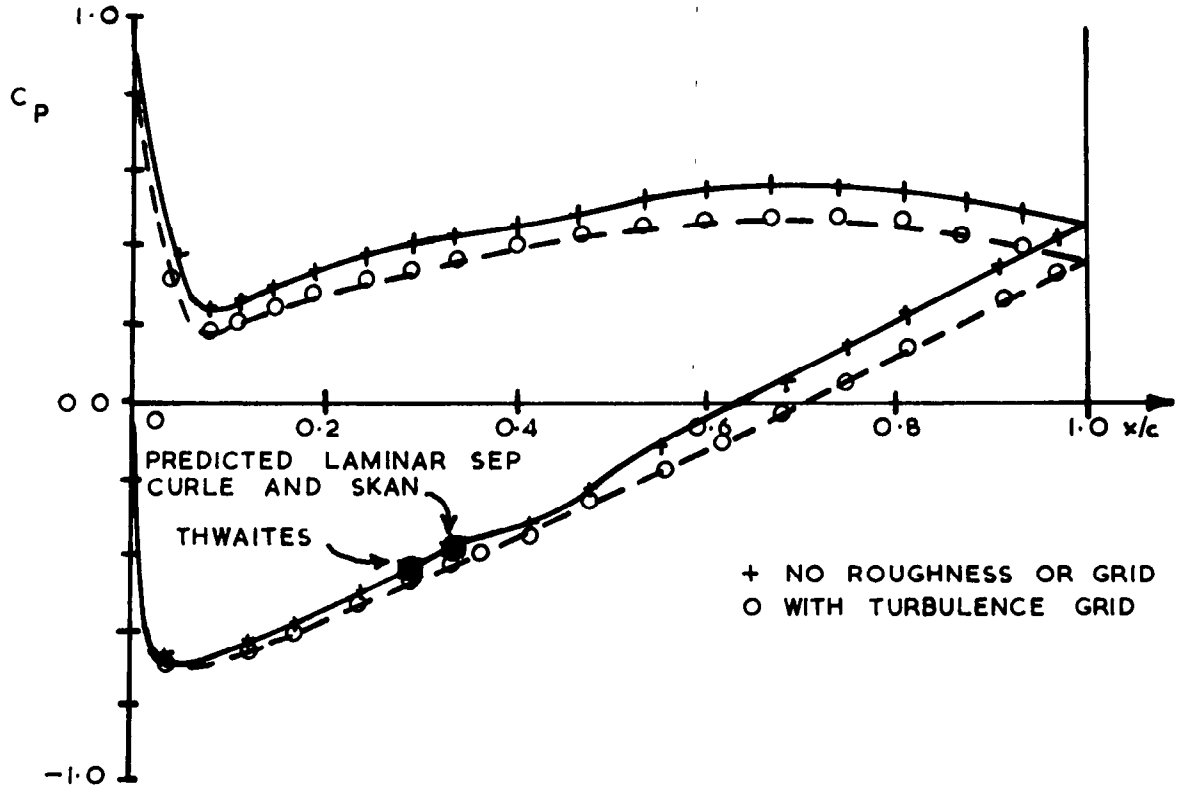

FIG. 13 PRESSURE DISTRIBUTIONS WITH AND WITHOUT UPSTREAM GRID

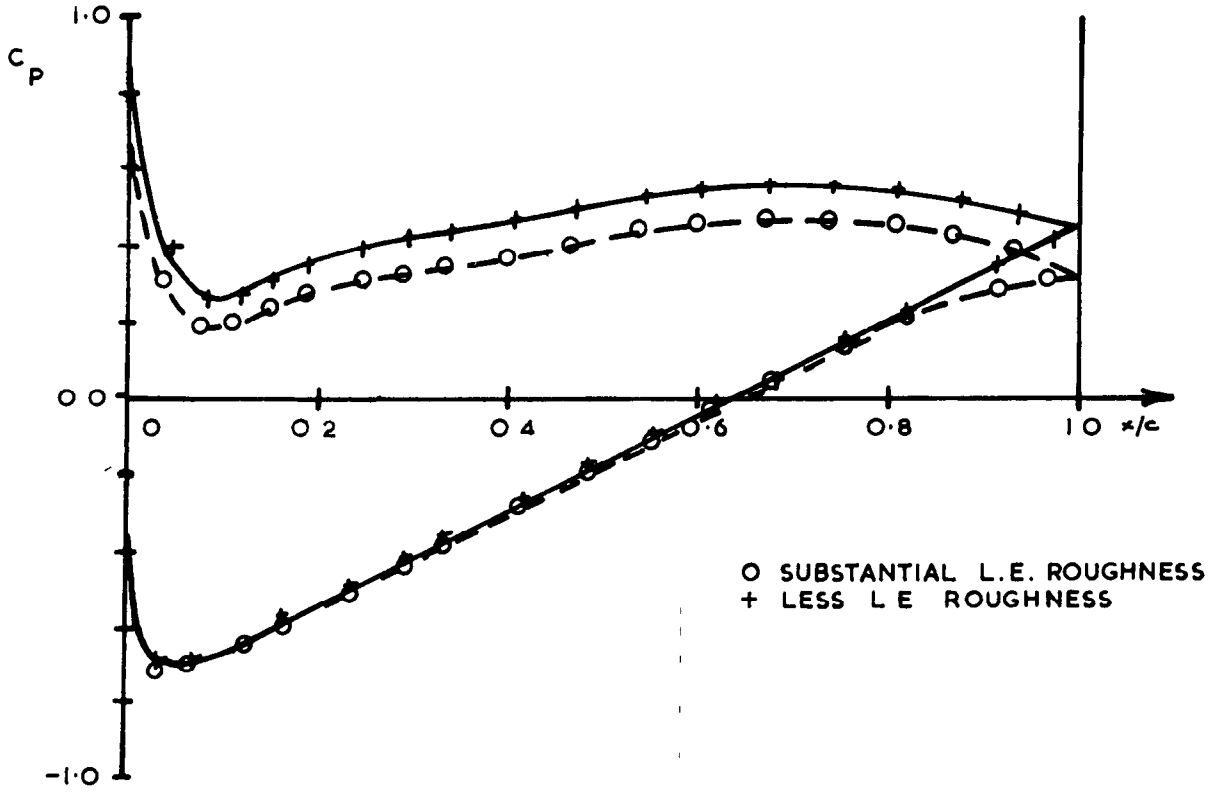

FIG. 14 PRESSURE DISTRIBUTIONS WITH LEADING EDGE ROUGHNESS

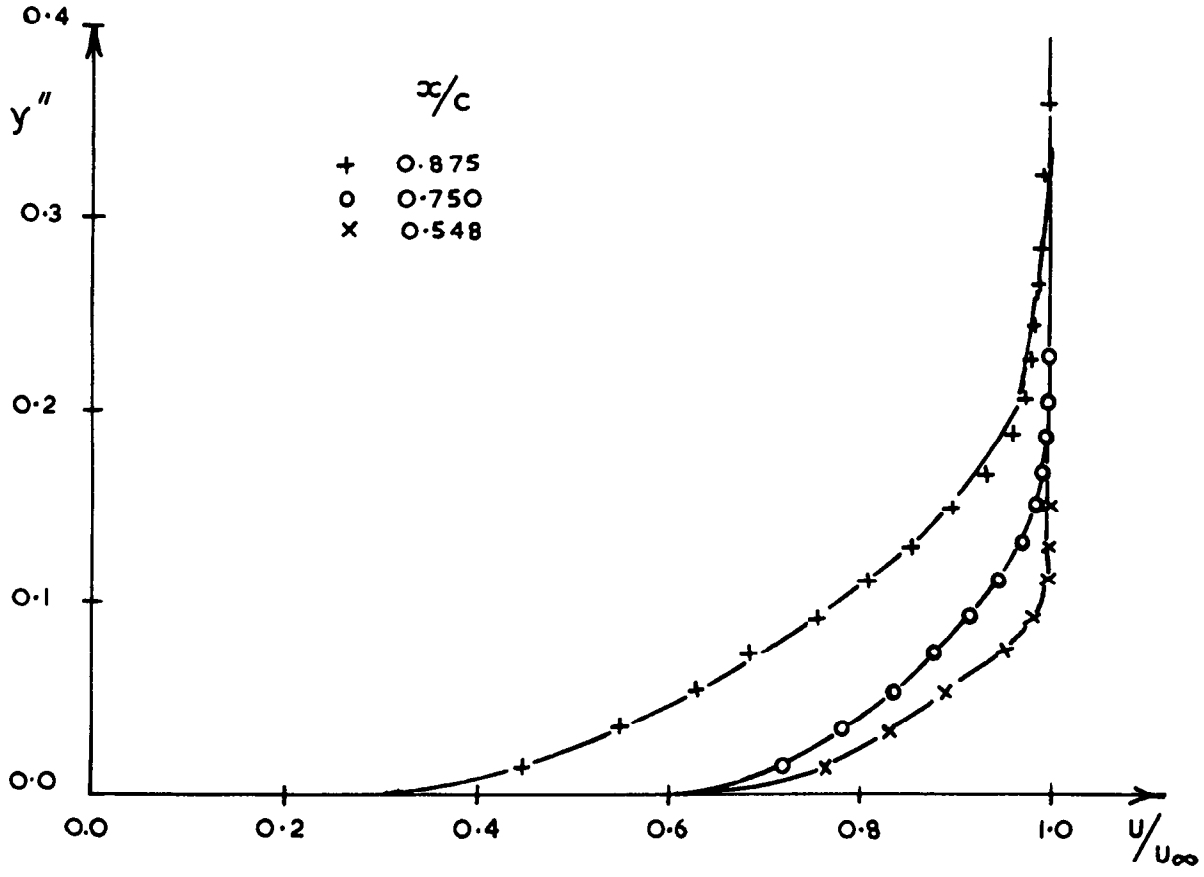

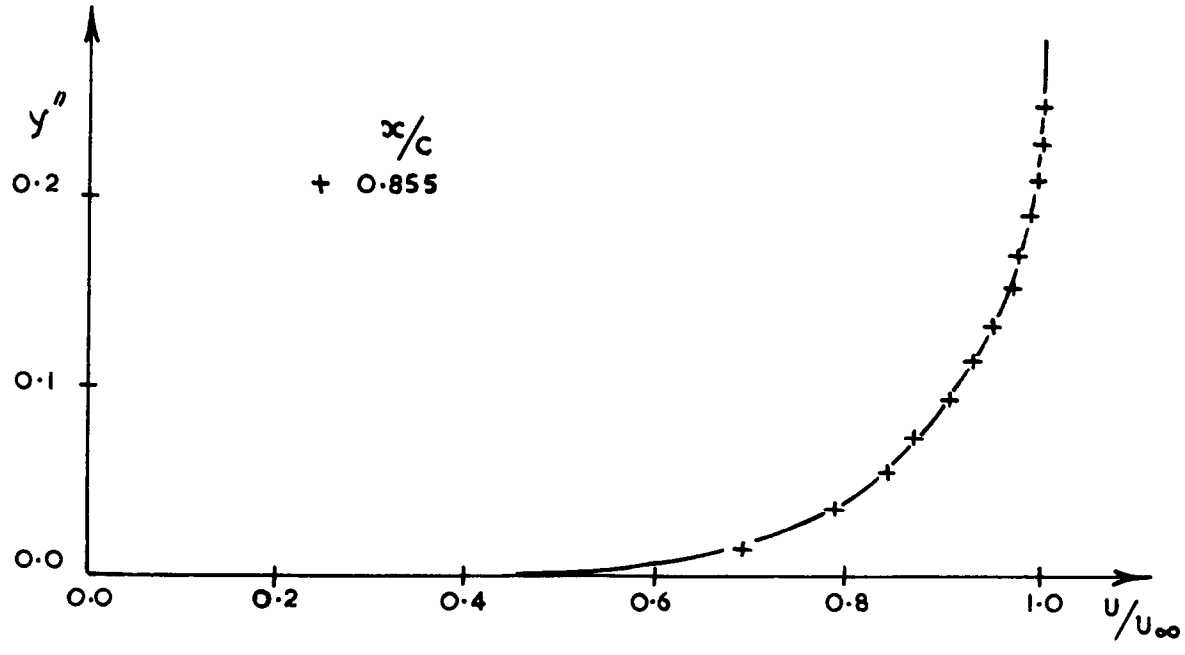

FIG.15 BOUNDARY LAYER TRAVERSES - NO ROUGHNESS.

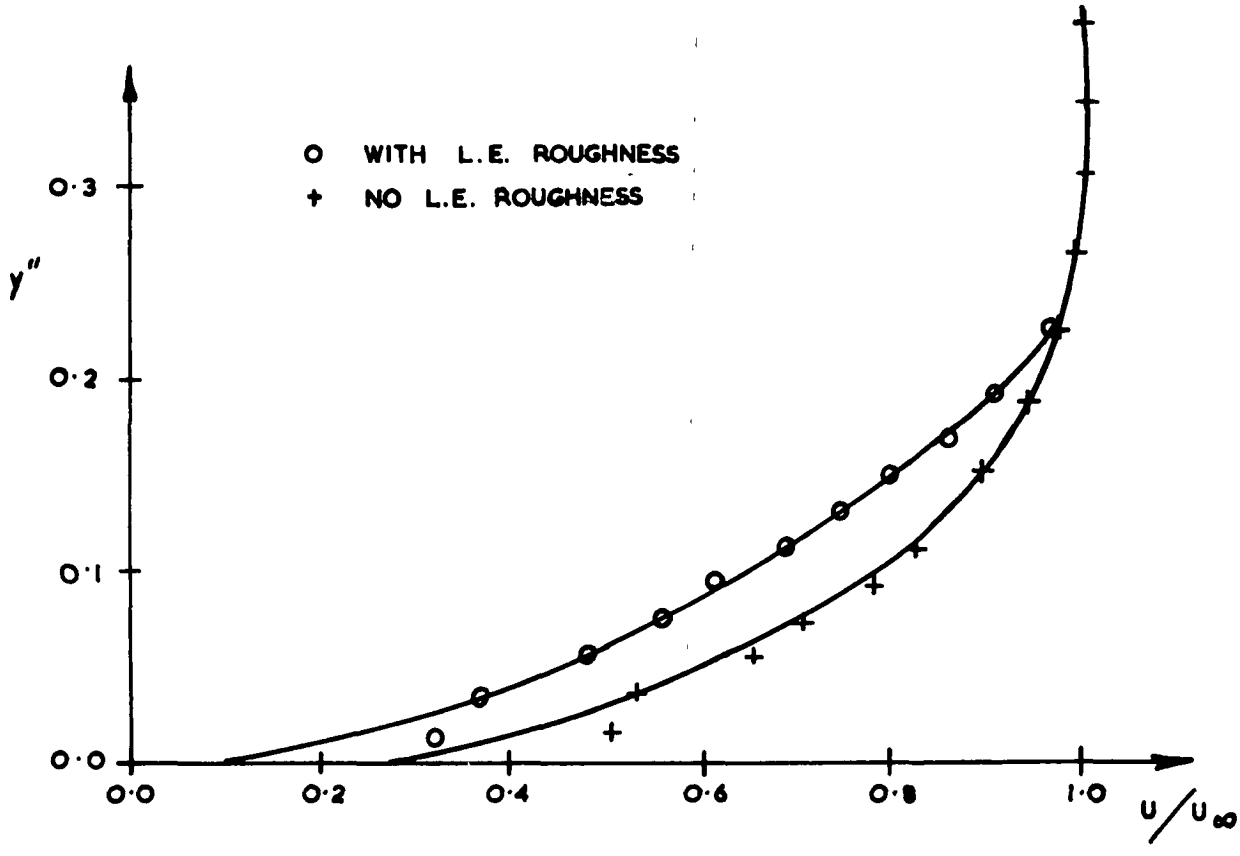

FIG. 16 BOUNDARY LAYER TRAVERSES — COMPARISON

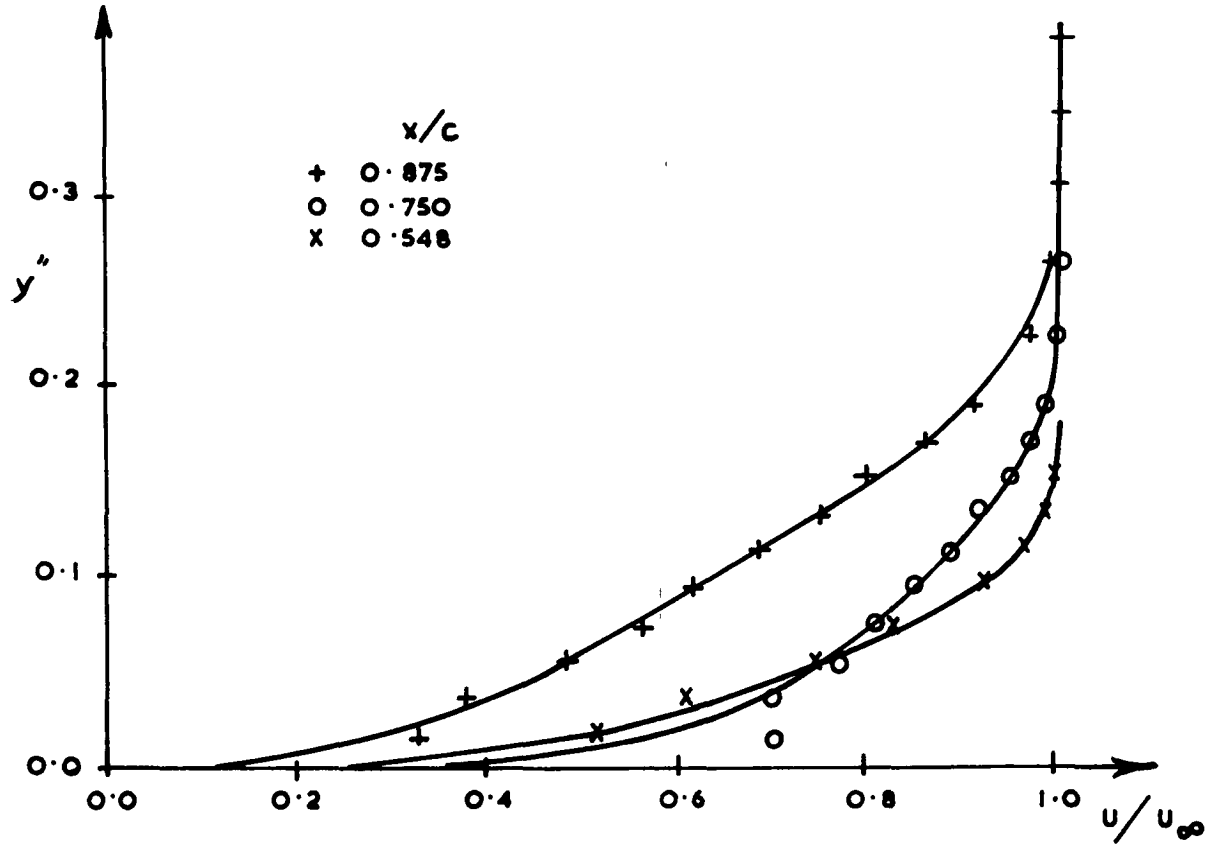

FIG. 17 BOUNDARY LAYER TRAVERSES — ROUGHNESS PRESENT.

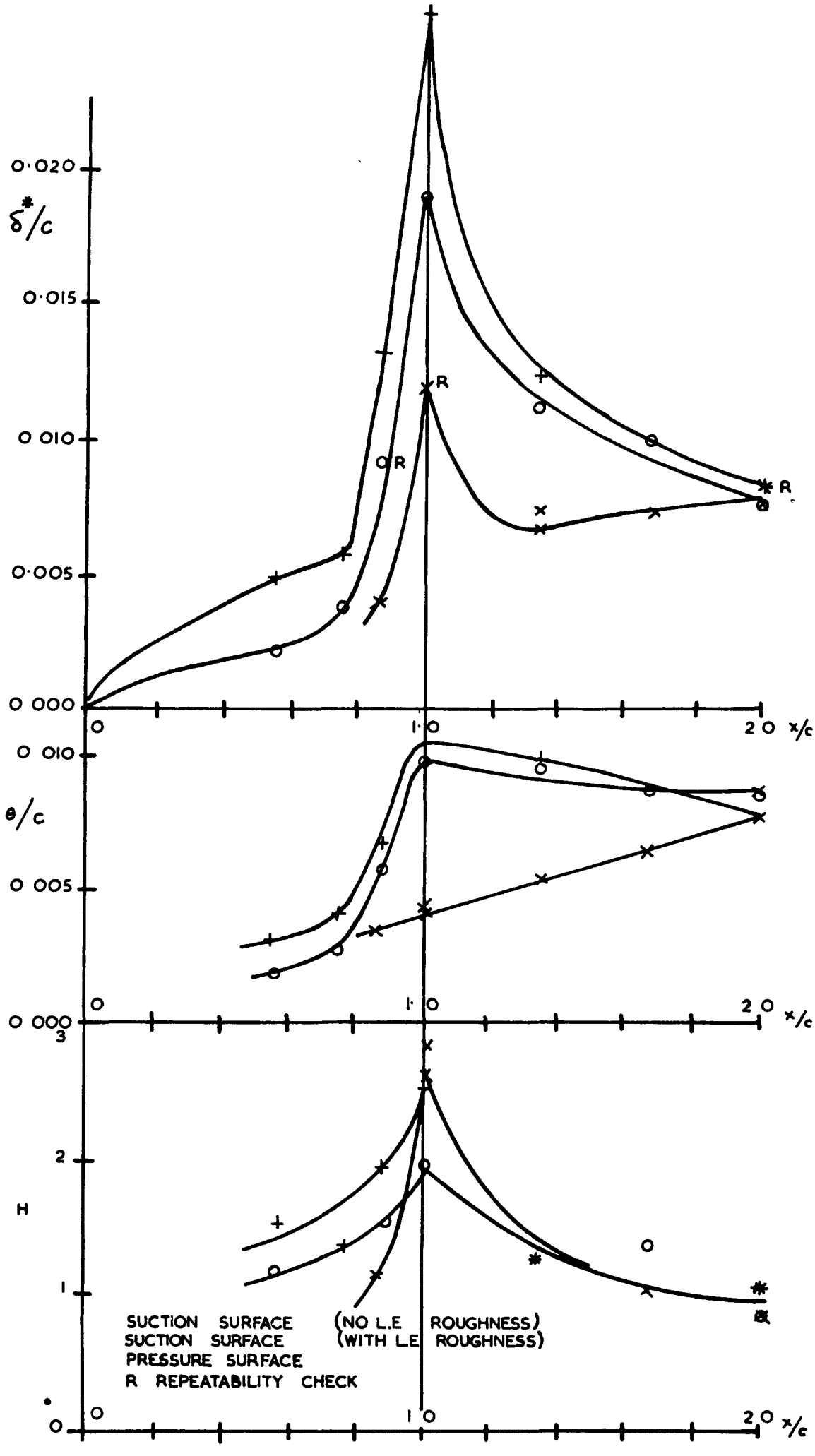

FIG. 18 EXPERIMENTAL BOUNDARY LAYER AND WAKE RESULTS.

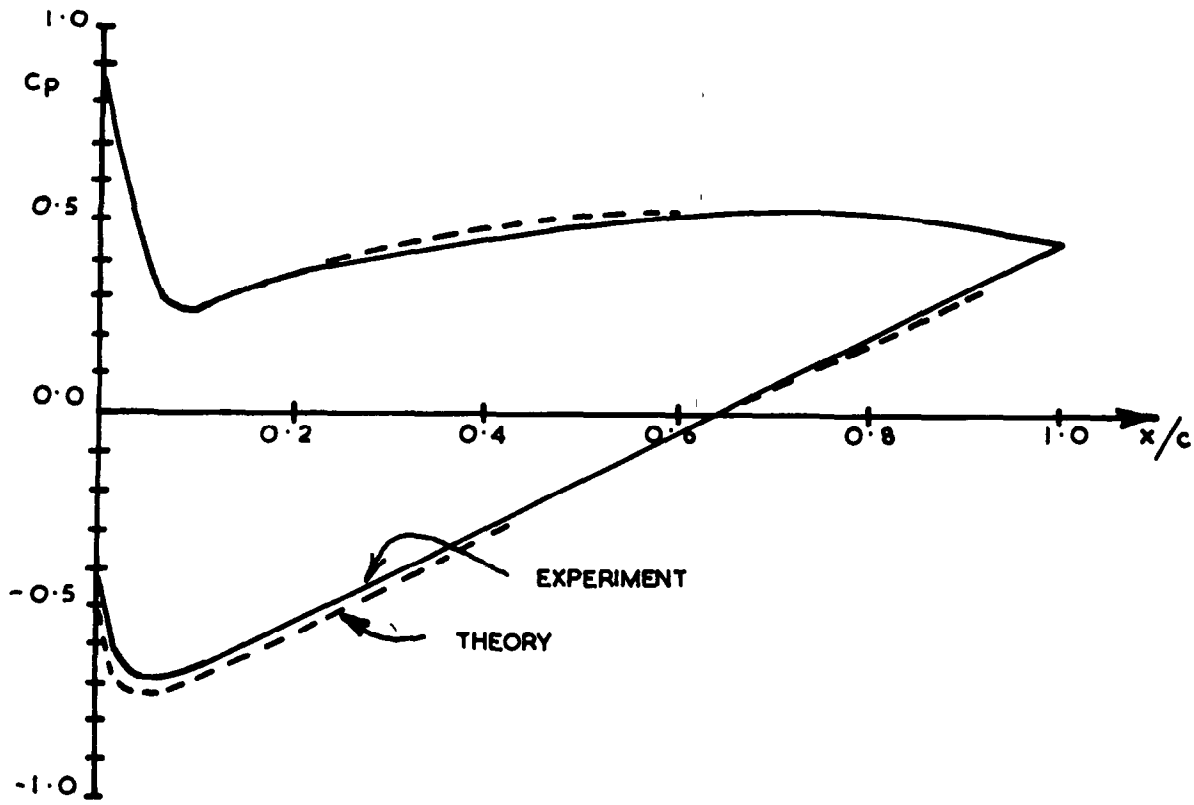

FIG. 19 COMPARISON BETWEEN EXPERIMENTAL AND THEORETICAL PRESSURE DISTRIBUTIONS.

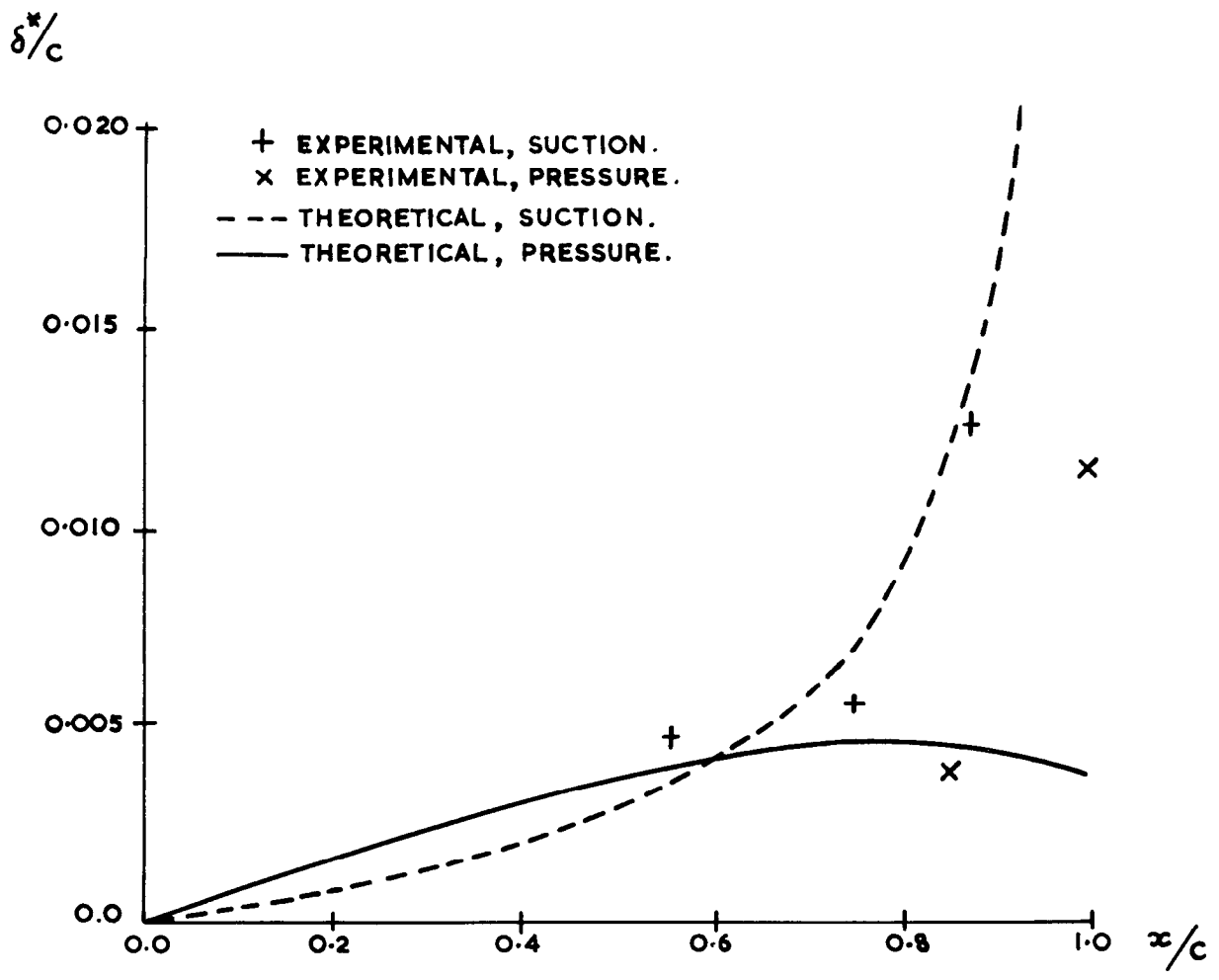

FIG.20 COMPARISON BETWEEN EXPERIMENTAL AND THEORETICAL BOUNDARY LAYER RESULTS. (DISPLACEMENT THICKNESS).

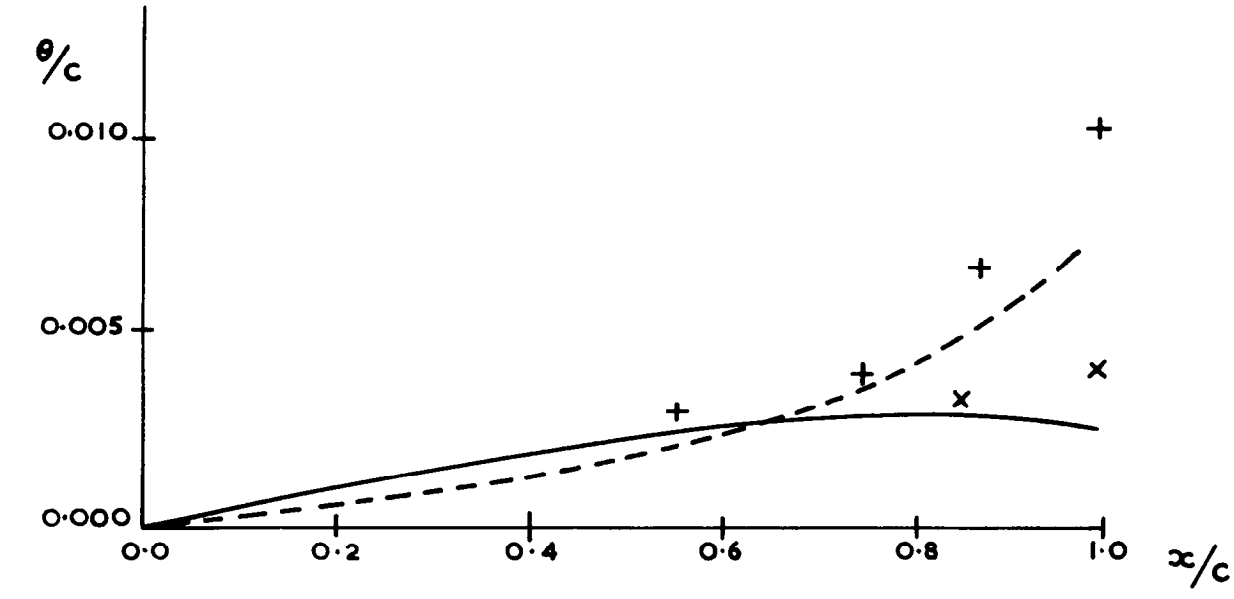

FIG.21 COMPARISON BETWEEN EXPERIMENTAL AND THEORETICAL BOUNDARY LAYER RESULTS. (MOMENTUM THICKNESS).

Printed and published by

HER MAJESTY'S STATIONERY OFFICE

To be purchased from
49 High Holborn, London W C 1
423 Oxford Street, London W 1
13A Castle Street, Edinburgh 2
109 St Mary Street, Cardiff
Brazennose Street, Manchester 2
50 Fairfax Street, Bristol 1
35 Smallbrook, Ringway, Birmingham 5
80 Chichester Street, Belfast 1
or through any bookseller

Printed in England

S.O Code No. 23-9016-72